

**Pilot Study for Internal Stem
Modelling:
Summary of Data collected
FR172/3**

J. C. Grace

Report No. 127 April 2006

Ensis Output

No. 39458

**Pilot Study for Internal Stem Modelling:
Summary of Data collected FR172/3**

J.C. Grace

**REPORT NO. 127
April 2006**

NOTE : Confidential to participants of the Stand Growth Modelling Cooperative.
: This is an unpublished report and must not be cited as a literature reference.

EXECUTIVE SUMMARY

A pilot study, to develop a data collection strategy for rotation age trials, was carried out in abandoned plots from Experiment FR172/3. Crown structure and wood property data were collected from 7 visually straight trees and 5 visually bent trees.

Data from the straight trees will be used to test an extension to TreeBLOSSIM, which predicts stem wood density from crown structure.

Images were taken of the wood samples. This was extremely valuable as it allowed us to compare the images with the measured wood properties. All the trees contained patches of visual compression, and it was obvious that density and microfibril angle increased, and longitudinal modulus of elasticity decreased in areas of visual compression wood.

The small number of trees sampled and the wide variability in the observed wood properties between individual trees made it difficult to draw any firm conclusions.

Based on these data, it is suggested that between 6 and 10 trees be destructively sampled from an individual seedlot in future studies. This intensive sampling should be augmented with less intensive and non-destructive sampling on a greater number of trees.

There were indications that different trees had different strategies for the formation/structure of wood, and that the relationships between different wood properties could vary.

Two approaches worth following to gain a better understanding of wood property variation in trees are:

- To examine branch wood properties to gain an understanding of how stem wood properties are likely to vary.
- To carry out manipulation studies on young plants in a greenhouse to determine what patterns of compression wood are formed by specific manipulations.

There is good knowledge of the general pattern of wood property variation within a tree. The underlying question that has not been well answered is:

What are the underlying causes that make trees form specific patterns of compression wood?

Research needs to be carried out to determine the impact of the observed variability in wood properties on wood property performance.

**PILOT STUDY FOR INTERNAL STEM MODELLING:
Summary of data collected in FR172/3**

J.C. Grace

Introduction

The objective of theme 4 (Internal Stem Modelling) within the Stand Growth Modelling Cooperative is:

- To develop and refine a tree-level model of internal wood properties with respect to stem shape and crown architecture, as well as, site, stocking, and planting stock.

For the same cost, studies of radiata pine wood properties could measure a few variables on a lot of trees, or a lot of different variables on a few trees. Generally the first approach is used. Since the variation in wood properties within a piece of timber can lead to problems with usage, it is considered that measuring more variables on a few trees will provide us with a better understanding of how tree growth influences wood formation, the resultant wood properties and their variability within a tree.

After the introduction of theme 4, the first project was a literature review (SGMC Report 114). The second project was this pilot study (carried out in experiment FR172/3, Kaingaroa). This pilot study followed the second approach mentioned above. Notable features of this study are features of this study are:

- A lot of variables were measured on a few trees.
- Tree growth and wood properties were measured concurrently on the same trees.
- The variability in wood properties around the stem was measured.
- It was designed to develop appropriate data collection procedures for future sampling in rotation-age trials.
- It was designed to provide a dataset to test the extension to TreeBLOSSIM that predicts ring width and wood density from crown structure (Pont, 2003).

The data collection procedures used in FR172/3 are documented in SGMC Report No. 126. In this report, the crown data and wood property data collected are summarised. An additional report will summarise the use of these data with TreeBLOSSIM.

Each tree has been given two unique identifiers, a combination of plot and tree number. In one case a letter is used for the plot, in the other case a number has been used for the plot. Seven of the trees were classified as “straight” while the other 5 were classified as “bent” (Table 1).

Table 1. Sample trees from Experiment FR172_3.

Seedlot	PlotID	Plot/ Tree Number	Unique Number	Tree DBH (mm)
Highly multinodal (GF27)	1	A5	105	381 (bent)
Highly multinodal (GF27)	1	A16	116	388
Highly multinodal (GF27)	1	A24	124	385
Long Internode (GF13 – LI25)	2	B24	224	354 (bent)
High wood density (GF18)	3	C9	309	349
High wood density (GF18)	3	C11	311	352 (bent)
Low wood density (GF28)	4	D9	409	326 (bent)
Low wood density (GF28)	4	D11	411	388
Low wood density (GF28)	4	D13	413	316
Gwavas seed orchard (GF14)	5	E16	516	318
Gwavas seed orchard (GF14)	5	E17	517	352
Gwavas seed orchard (GF14)	5	E22	522	318 (bent)

Several of the analyses were carried out using the SAS[®] procedure PROC GLM. This procedure uses the method of least squares to fit mathematical equations to observed data. Both continuous variables (such as mean top height and basal area) and class variables (such as site and treatment) may be included in the equation as independent variables. An illustrative example equation is:

$$y = c + a_1x_1 + a_2x_2 + \sum_i b_{1i}z_{1i} + \sum_j b_{2j}z_{2j}$$

Where:

- y is the dependent variable to be predicted
- c is the model intercept
- x_1, x_2 are continuous variables
- a_1, a_2 are the model parameters associated with the continuous variables
(actual predicted values are the model coefficients)
- z_1, z_2 are class variables. These have the value 1 if the data corresponds to that class,
otherwise the value is zero
- b_{1i}, b_{2j} are the model parameters associated with the class variables
(actual predicted values are model coefficients)

One statistic calculated is the ‘Least Square Mean’. This is an estimate of the class mean that would have been expected if the design were balanced. In the case of a balanced design it corresponds to the arithmetic mean.

Crown Structure – Number of clusters in an annual shoot

Data available

The position of branch clusters was measured for each tree. Stem growth rings were counted above and below each branch cluster on each tree. Ring counts were only available for approximately the lower third of the clusters from trees 105 and 311.

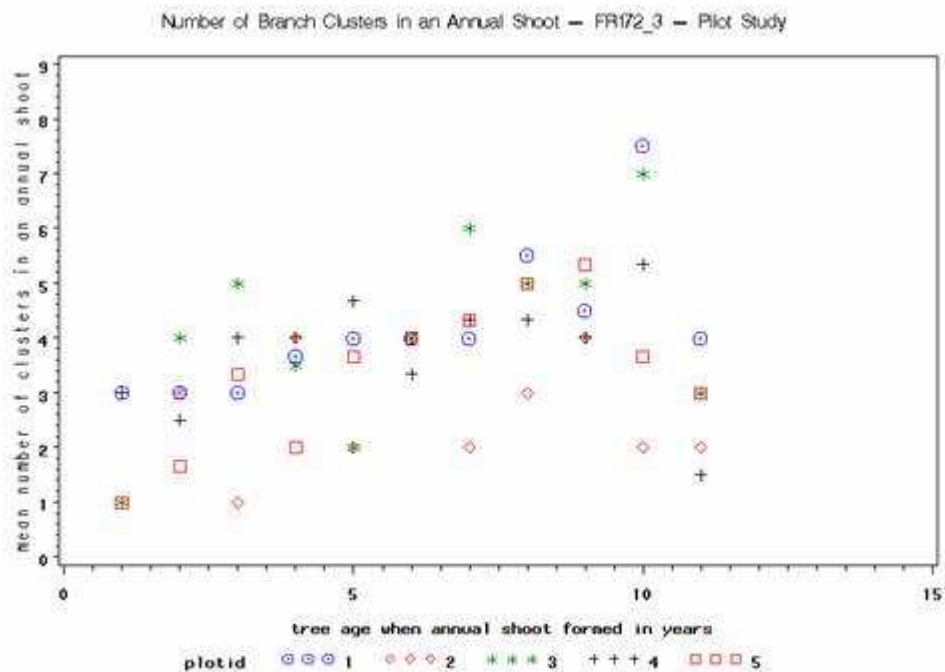
Assuming that height growth was complete for the 2002/3 growing season (trees measured in March 2003), this equated to 106 complete annual shoots with between 1 and 9 branch clusters per annual shoot.

The data recorded indicated that one annual shoot in Tree 124 contained nine branch clusters. This is higher than has been observed in any previous branch study, and occurred when the tree age was 10 years. Other trees also formed a high number of branch clusters in this year. Given that tree 124 was from a highly multinodal seedlot, it is considered that it is more likely to be real than an error in counting stem growth rings.

Data Analysis

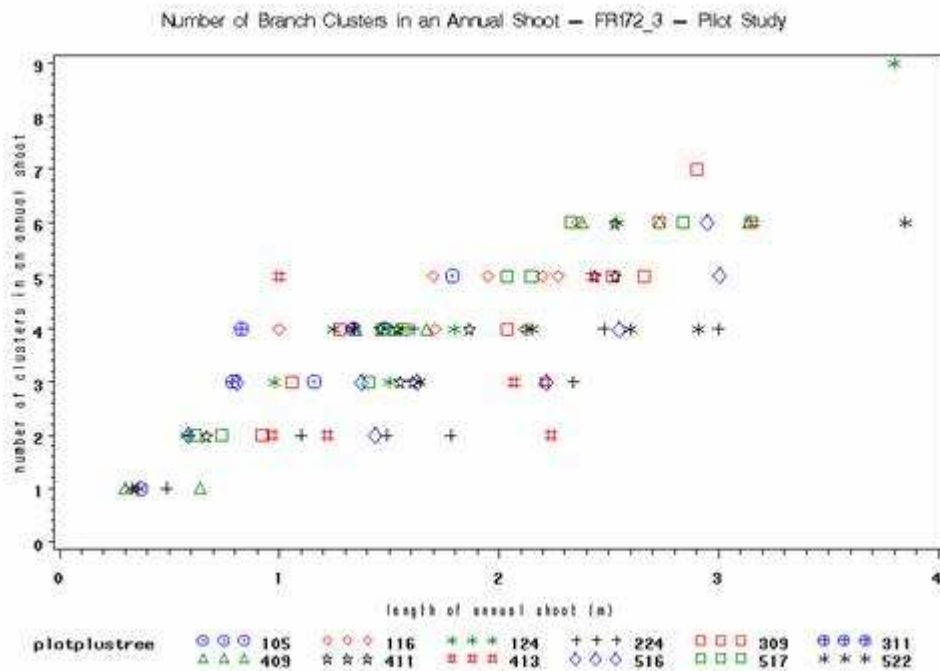
Previous studies (e.g. Bannister, 1962) have indicated that the number of branch clusters per annual shoot tended to increase towards an asymptote with increasing tree age. The same pattern has been observed in this study (Figure 1). These data also indicate that height growth for the 2002/3 growing season (tree age = 11 years) might not be complete, as the mean number of clusters formed per year tended to be lower than previous years.

Figure 1. Mean number of branch clusters in an annual shoot for each seedlot (plotid) sampled (all trees included).



As observed in other SGMC studies, the number of branch clusters in the annual shoot increased with increasing annual shoot length (Figure 2).

Figure 2. Observed relationship between number of branch clusters in the annual shoot and annual shoot length.



Note: ‘plotplustree’ is the unique number given to each tree in Table 1.

The relationship between number of clusters in an annual shoot and shoot length appears linear. The SAS procedure, PROC GLM, was used to investigate whether annual shoot length, seedlot (plot), tree within seedlot, and stem form had a significant effect on the number of branch clusters in an annual shoot. Only shoot length and seedlot were significant, i.e. for a given shoot length, the number of branch clusters in an annual shoot varies with seedlot. The mean number of branch clusters in an annual shoot for each seedlot is shown in Table 2. The least square means ranges from 3.1 (long internode seedlot) to 4.6 (highly multinodal seedlot).

It is possible that the result would be different with a bigger sample of trees. There are differences between individual trees from the same seedlot (Table 3). Of interest is the observation that the bent trees have at least 1 annual shoot with only 1 cluster (Figure 3).

Table 2. Least Square Mean values for the number of branch clusters in an annual shoot for each seedlot (excluding age 11 data and two trees with incomplete ring counts)

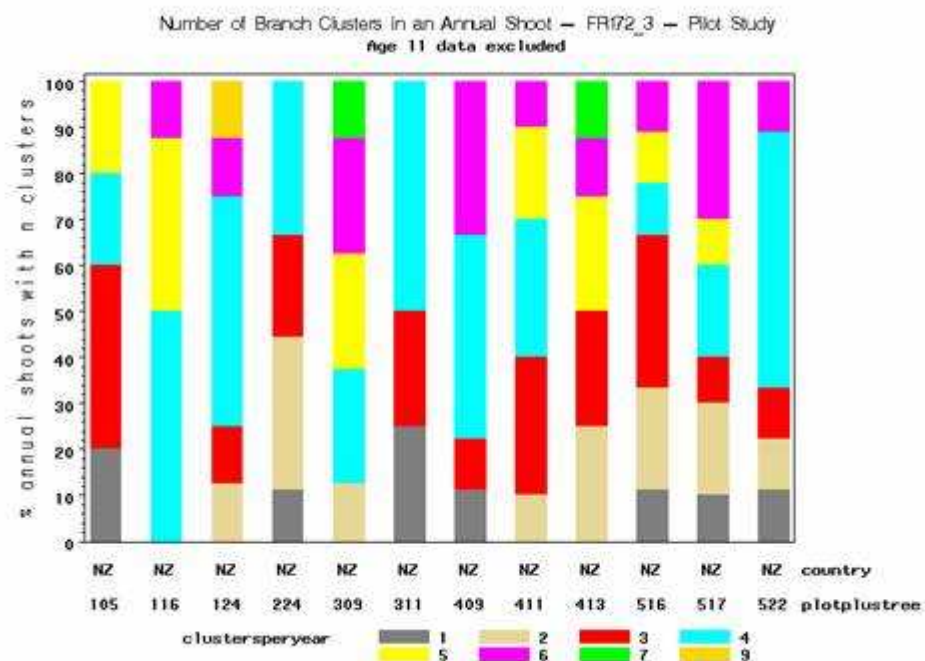
Seedlot	Plotid	Least Square Mean
Highly multinodal (GF27)	1	4.6
Long Internode (GF13 – LI25)	2	3.1
High wood density (GF18)	3	4.3
Low wood density (GF28)	4	4.0
Gwavas seed orchard (GF14)	5	3.8

Table 3. Mean number of clusters per annual shoot for each tree (age 11 data excluded)

Seedlot	Plotplustree	Tree DBH (cm)	Mean number of clusters per annual shoot
Highly multinodal (GF27)	105	381 (bent)	3.2
Highly multinodal (GF27)	116	388	4.6
Highly multinodal (GF27)	124	385	4.5
Long Internode (GF13 – LI25)	224	354 (bent)	2.8
High wood density (GF18)	309	349	4.9
High wood density (GF18)	311	352 (bent)	3.0
Low wood density (GF28)	409	326 (bent)	4.2
Low wood density (GF28)	411	388	3.9
Low wood density (GF28)	413	316	4.1
Gwavas seed orchard (GF14)	516	318	3.2
Gwavas seed orchard (GF14)	517	352	3.9
Gwavas seed orchard (GF14)	522	318 (bent)	3.6

Note: Ring counts were incomplete for trees 105 and 311. This has influenced mean number of clusters per year.

Figure 3. Frequency distribution for number of branch clusters in an annual shoot.



Note: Ring counts were missing for the top part of trees 105 and 311.

Crown Structure – Number of branches and number of cones in a cluster

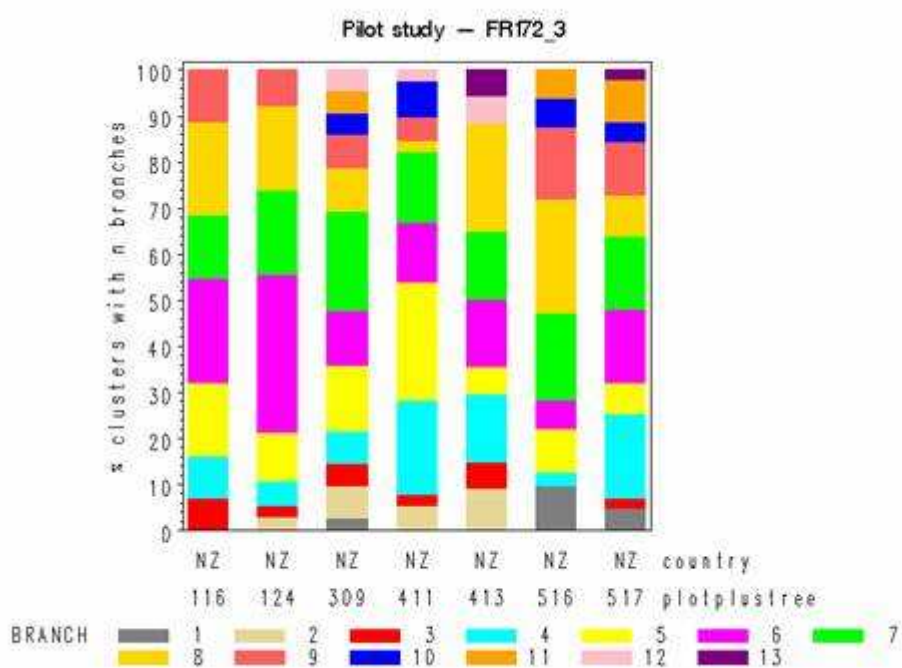
Data available

Counts of the number of branches and number of cones in a cluster are available for the 7 straight trees, a total of 273 clusters. The data set is incomplete for the bent trees, and these data have not been included in the analysis below.

Data Analysis

The number of branches in a cluster varied from 1 to 13 (Figure 4). The number of branches in a cluster did not vary significantly between plots or between trees within plots. The mean number of branches in a cluster (least square mean values) varied between 6.2 and 6.9 for the different seedlots (Table 4). There were very few clusters with stem cones (Figure 5). This is considered to be due to the fact the trees are only 11 years old, and trees do not produce stem cones for the first few years of their life.

Figure 4. Frequency distributions for the number of branches in a cluster (straight trees).

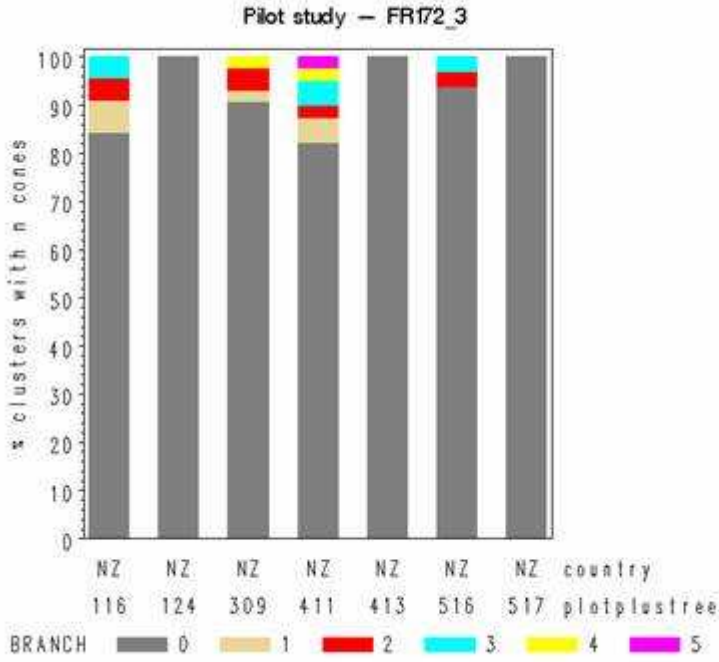


Note: “branch” refers to the number of branches in a cluster

Table 4. Mean (least square means) number of branches in a cluster (straight trees)

Plot	Number of sample trees	Mean number of branches in a cluster
A – Highly multinodal	2	6.4
C – High wood density	1	6.5
D – Low wood density	2	6.2
E – Gwavas seed orchard	2	6.9

Figure 5. Frequency distributions for the number of cones in a cluster (straight trees).



Note: “branch” refers to the number of cones in a cluster

Crown Structure – Branch foliage

Data available

The two crown characteristics that are used to estimate wood properties (Pont, 2003) are:

- Distance to foliage
- Foliage mass

To this end the following variables, suggested by D. Pont, were measured on a selection of branches:

- Branch weight with foliage present
- Distance to centre of gravity of branch with foliage present
- Branch weight with foliage removed
- Distance to centre of gravity of branch with foliage removed

Seven or eight branches were measured from each straight tree, covering a range of branch diameter and branch age. All up data were available for 53 branches.

Data Analysis

The foliage weight on a branch increased rapidly with increasing branch diameter (Figure 6). These trees were only 11 years old. It is considered that the relationship would be ‘bell-shaped’ for older trees, because the amount of foliage on a branch will decrease as the branch becomes moribund, whereas the branch diameter will remain approximately constant.

The distance to foliage increased linearly with increasing branch diameter (Figure 7). It is possible that this relationship will not be linear if older branches were included, because the distance to foliage would be increasing whilst the branch diameter remained approximately constant.

There was no significant effect of seedlot on either relationship.

Figure 6. Relationship between foliage weight and branch diameter adjacent to the stem

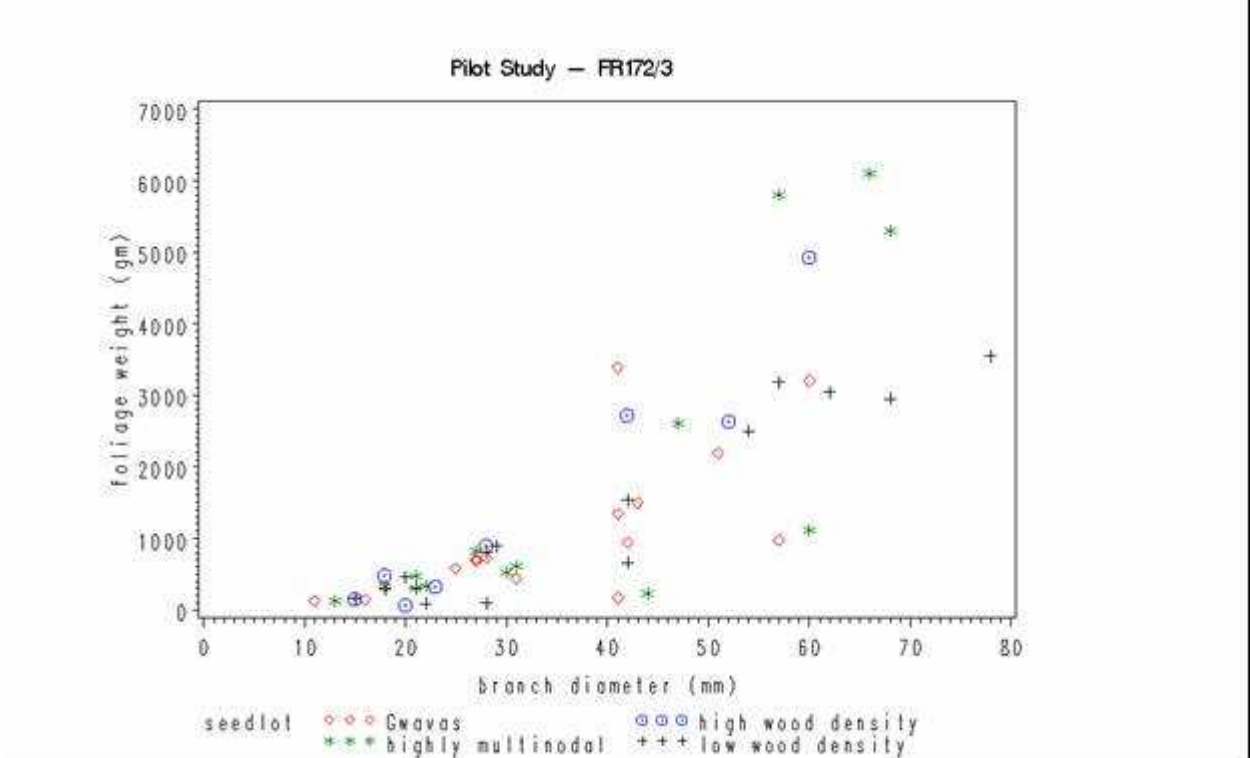
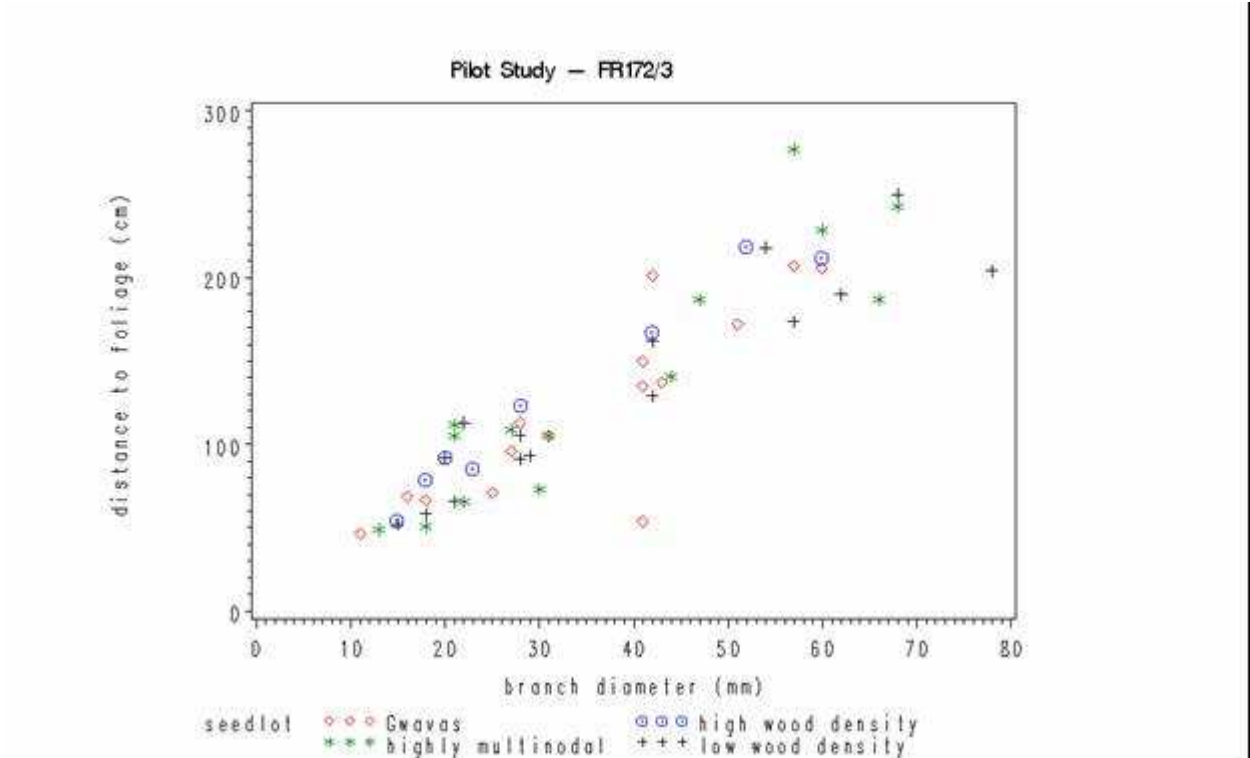


Figure 7. Relationship between distance to foliage and branch diameter adjacent to the stem.



Wood Properties – Spiral Grain

Spiral grain variation within a tree is possibly not as well understood as density variation within a tree. Spiral grain influences timber distortion (Ormarsson, 1999). Spiral grain generally decreases with ring number from the pith (Harris and Cown, 1991). An analysis by Skatter and Archer (unpublished) indicated that a tree would survive better with varying grain angle compared to a uniform grain angle.

Data available

Spiral grain was measured at 5 levels in 6 of the straight trees, 4 levels in the 7th straight tree and 2 levels for 2 of the bent trees.

Data Analysis

The minimum, maximum and mean spiral grain for individual trees is shown in Table 5. The least square means are calculated using tree, tree age at time ring was formed and ring number from the pith as class variables. Graphs of the data for individual trees are shown in Appendix 1.

Table 5. Observed minimum, maximum and mean spiral grain for individual trees.

Seedlot	Unique Number	Number Obs.	Minimum Spiral Grain (degrees)	Maximum Spiral Grain (degrees)	Arithmetic Mean Spiral Grain (degrees)	Least Square Mean Spiral Grain (degrees)
Straight trees						
Highly multinodal (GF27)	116	72	-4.0	11.0	3.7	2.3
Highly multinodal (GF27)	124	74	0.0	15.0	6.5	5.3
High wood density (GF18)	309	65	0.5	12.0	5.3	3.8
Low wood density (GF28)	411	75	0.0	13.0	5.7	4.6
Low wood density (GF28)	413	44	0.0	9.0	3.6	1.6
Gwavas seed orchard (GF14)	516	67	-1.5	13.0	4.9	3.3
Gwavas seed orchard (GF14)	517	83	-3.5	11.0	6.1	4.8
Bent trees						
Highly multinodal (GF27)	105	29	2.0	17.5	8.3	6.0
High wood density (GF18)	311	26	2.0	10.0	7.2	4.7

Within an individual tree, spiral grain varied by up to 15.5 degrees. The least square means for the individual trees varied between 1.6 degrees and 5.3 degrees. The least square means differed by 3 degrees for the two straight trees from both the highly multinodal and low wood density seedlots.

Wood Properties – SilviScan data

The wood within a tree is not all the same. Compression wood, which tends to be visually darker, is known to have different cell structure and consequently different wood properties from ‘normal’ / ‘non-compression’ wood (e.g. Harris, 1977). These differences in cell structure affect the gross properties of compression wood compared with ‘normal wood’:

- The wood density is higher.
- The longitudinal modulus of elasticity is lower.
- It has greater longitudinal shrinkage but less transverse shrinkage.
- The relationship between microfibril angle and shrinkage is different.

SilviScan is a tool, developed by CSIRO, which measures various wood properties.

Three processes are used to provide data:

- X-ray to provide data on wood density
- Diffraction to provide data on microfibril angle
- Image analysis to provide data on cell properties

Various other properties can be estimated from these data, for example, longitudinal modulus of elasticity.

Data available

For this study:

- Density was measured at 50 micron radial steps
- MFA was measured at 5 mm radial steps
- MOE was estimated at 5 mm radial steps
- Cell properties were measured at 50 micron radial steps

The data has been split into several groups for analysis.

- 1 To investigate how crown structure influences wood properties:
 - Density, MFA, MOE and cell properties are available for 84 strips (10 to 14 strips from each straight tree).
- 2 To investigate how stem form influences wood properties:
 - Density, MFA, and estimated MOE available for 12 strips (6 strips from each of 2 bent trees).
- 3 To investigate how wood shrinkage is related to wood properties:
 - Density, MFA, MOE and cell properties are available for 20 strips (4 strips from the base of the each bent tree).
- 4 To investigate how wood properties vary within an internode
 - density, MFA, and estimated MOE available for 74 strips (6 – 12 strips from one internode from each straight tree).

- 5 To investigate how wood properties vary within a swept internode
 - Density, MFA, and estimated MOE available for 16 strips (8 strips from one swept internode for two of the bent trees).
- 6 To investigate how wood properties vary within a branch
 - Density, MFA, and estimated MOE available for 26 strips (2 strips from each of 13 branches).

Images were taken of adjacent samples allowing us to compare how wood properties changed with visual colour.

Note:

It is only possible to obtain 2 pith-bark samples from any disc. For strips that do not include the pith, the ring nearest the pith may be incomplete. In the data analysis and graphs, it has been assumed that this ring is complete. From the graphs plotted, this assumption does not appear to have a major affect on the values of wood properties.

Data analysis (Group 1)

This group consisted of 84 strips (10 to 14 strips from each straight tree).

Graphs of the data for the individual straight trees are given in Appendix 1 (Tables 15-21). The layout of these Tables is shown in Table 14. The images of the wood samples indicate that all the straight trees contained patches of visual compression wood. Comparing the SilviScan data with the images, it is clear that visual compression wood does have an influence on the wood properties. The unanswered question is what made the trees form compression wood in these places.

The minimum, mean and maximum for the ring-average values of density, microfibril angle and longitudinal modulus of elasticity as measured by SilviScan are shown in Table 6, Table 7, and Table 8 respectively. The least square means were calculated using tree, tree age at time ring was formed and ring number from the pith as class variables in the SAS procedure PROC GLM. The relationship between the least square mean values of wood properties and tree DBH are shown in Table 9. There was no significant relationship between tree DBH and these wood properties. However it needs to be considered that these trees were from a range of different seedlots. Trees 116 and 413 stand out as having a high density, low microfibril angle and high MOE for their DBH. Tree 413 also had very variable wood properties, which could be a disadvantage in sawn timber. A larger sample size will be needed to draw any comparisons between the different seedlots.

Assuming these trees were from an infinite random population, the following equations can be used to estimate an appropriate sample size.

The confidence interval for the mean of a variable is:

$$\bar{y} \pm ts_y \quad \text{Eqn. 1}$$

where:

\bar{y} is the mean

s_y is the standard error of the mean

t is an appropriate t-value

The standard error of the mean is calculated from the variance of the sample as:

$$s_y^2 = \frac{s_y^2}{n} \quad \text{Eqn. 2}$$

where:

n is the sample size

s_y^2 is the variance of the sample

Assuming that we would like the error to be less than or equal a given value E , then an appropriate sample size can be calculated by setting E equal to the confidence interval, i.e.

$$E = ts_y \quad \text{Eqn. 3}$$

$$E^2 = t^2 \frac{s_y^2}{n} \quad \text{Eqn. 4}$$

Hence the sample size, n , is given by:

$$n = \frac{t^2 s_y^2}{E^2} \quad \text{Eqn. 5}$$

In this case:

\bar{y} was calculated as the mean of the individual tree least square means for each wood property.

E was set to 5% of the mean value of the individual tree least square means for each wood property.

The estimated sample size required for each wood property was:

Spiral grain:	>200
Wood Density:	6
Microfibril angle:	9
Modulus of Elasticity:	70

From these results, and given the time involved to destructively sample 1 tree, it is suggested that:

- 6 and 10 trees are sampled from an individual seedlot (treatments) in future studies.

This intensive sampling should be augmented with less intensive and non-destructive sampling on a greater number of trees.

Table 6. Minimum, mean and maximum values for ring average density (kg m^{-3}) for each straight tree.

Seedlot	Unique Number	Number Obs.	Minimum Density	Maximum Density	Arithmetic Mean Density	Least Square Mean Density
Highly multinodal (GF27)	116	74	341	542	436	459
Highly multinodal (GF27)	124	75	313	594	393	417
High wood density (GF18)	309	70	331	473	393	418
Low wood density (GF28)	411	77	327	469	398	420
Low wood density (GF28)	413	46	352	527	424	467
Gwavas seed orchard (GF14)	516	70	344	601	432	458
Gwavas seed orchard (GF14)	517	89	347	513	406	431

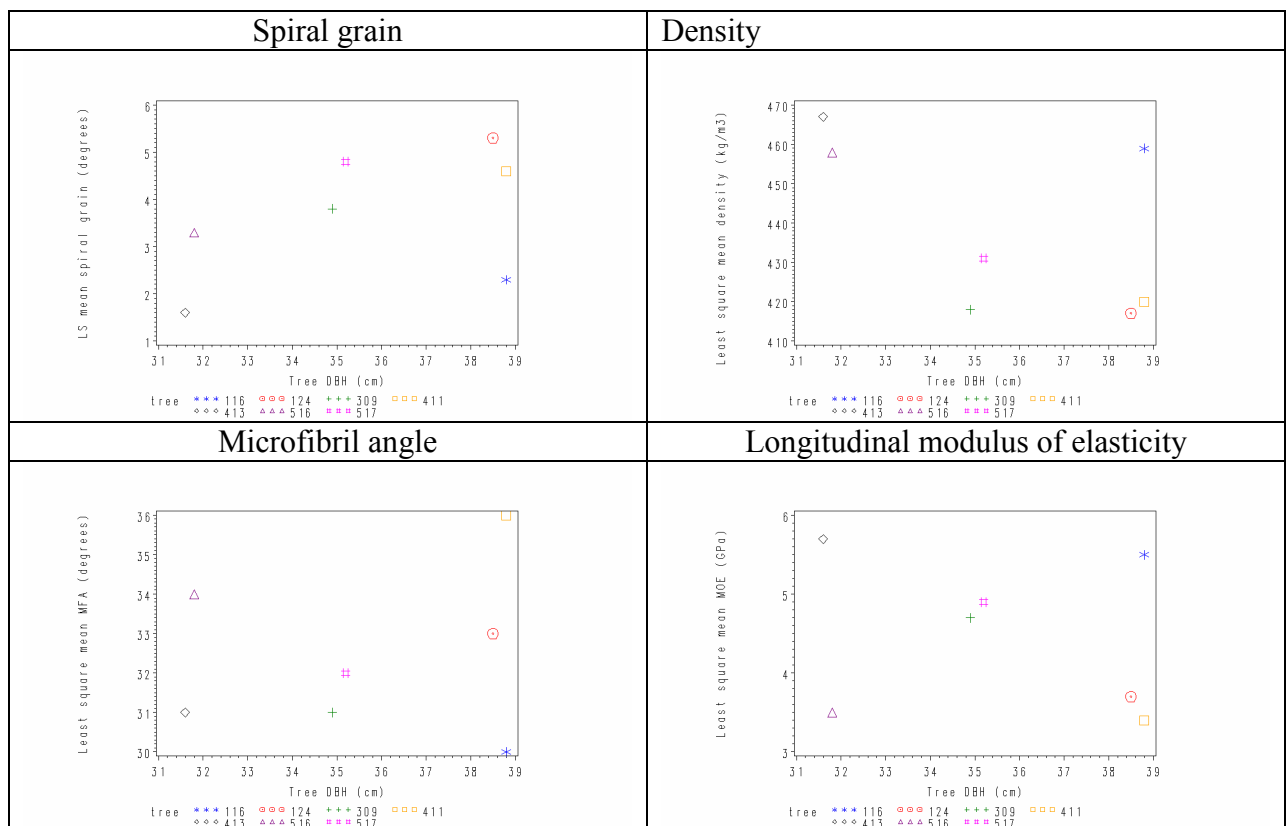
Table 7. Minimum, mean and maximum values for microfibril angle (degrees) for each straight tree.

Seedlot	Unique Number	Number Obs.	Minimum MFA	Maximum MFA	Arithmetic Mean MFA	Least Square Mean MFA
Highly multinodal (GF27)	116	74	20	33	27	30
Highly multinodal (GF27)	124	75	21	49	29	33
High wood density (GF18)	309	70	15	44	27	31
Low wood density (GF28)	411	77	25	40	33	36
Low wood density (GF28)	413	46	17	34	26	31
Gwavas seed orchard (GF14)	516	70	20	44	31	34
Gwavas seed orchard (GF14)	517	89	21	42	29	32

Table 8. Minimum, mean and maximum values for ring-average longitudinal modulus of elasticity (GPa) for each straight tree.

Seedlot	Unique Number	Number Obs.	Minimum MOE	Maximum MOE	Arithmetic Mean MOE	Least Square Mean MOE
Highly multinodal (GF27)	116	74	3.3	9.4	6.1	5.5
Highly multinodal (GF27)	124	75	1.0	6.4	4.3	3.7
High wood density (GF18)	309	70	1.9	9.4	5.4	4.7
Low wood density (GF28)	411	77	2.0	6.0	3.9	3.4
Low wood density (GF28)	413	46	3.4	10.7	6.8	5.7
Gwavas seed orchard (GF14)	516	70	1.4	8.5	4.2	3.5
Gwavas seed orchard (GF14)	517	89	1.7	8.1	5.6	4.9

Table 9. Relationship between least square mean values of wood properties and tree DBH.



Data Analysis (Group 2)

This group consisted of 12 strips (6 strips from each of 2 bent trees, A05 and C11). The lower discs were from approximately 5 m, and the higher disc from approximately 10 m. Graphs of the data for individual trees are given in Appendix 2, Tables 23-24. The layout of these Tables is shown in Table 22. While these two trees contained visual compression wood, there was not obviously more than in the straight trees.

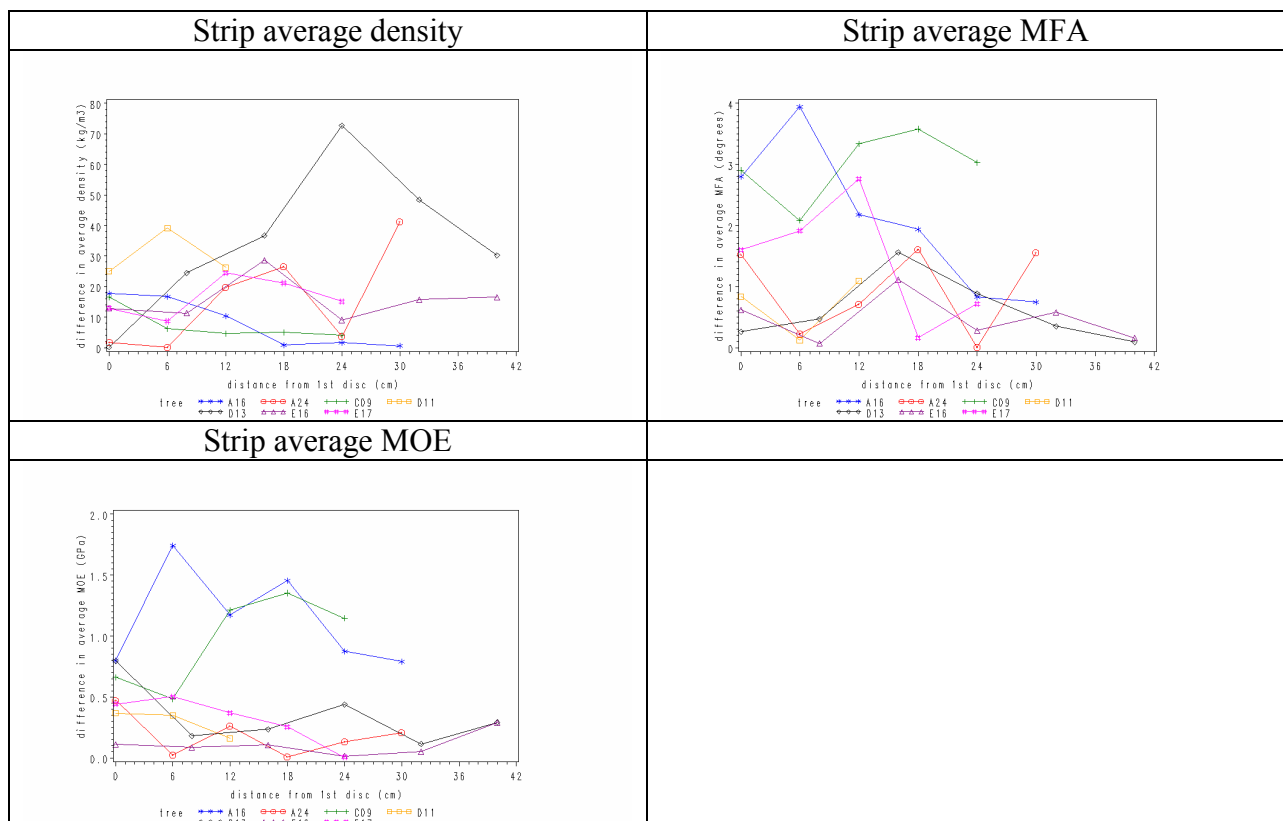
The PhotoMARVL image for tree C11 (Appendix 7) indicated that the tree was visually straight apart from butt sweep. The PhotoMARVL image of tree A05 indicated that the tree was reasonably straight. Hence the lack of compression wood in these samples is not unexpected.

Data analysis (Group 4)

This group consisted of 74 strips (6 – 12 strips from one internode from each straight tree). Graphs of the data for individual trees are given in Appendix 3, Tables 26-30. The layout of these Tables is shown in Table 25. The different internodes exhibit different patterns of visual compression wood.

The absolute difference in strip average density, MFA and MOE was calculated for the two strips on the same disc and plotted against distance from disc nearest the branch cluster (Table 10). The two trees from the low wood density seedlot exhibited the greater variation in density, while trees A16, and C09 exhibited the greater variation in MFA and MOE.

Table 10. Absolute difference in strip average wood properties for samples from the same wedge versus distance from wedge nearest the branch cluster.



Data analysis (Group 5)

This group consisted of 16 strips (8 strips from one swept internode for two of the bent trees). Graphs of the data for individual trees are shown in Appendix 4, Tables 32-33. The layout of these Tables is shown in Table 31. As with other groups of samples, differences in wood properties appeared to be related to differences in visual colour. For tree E22, the visual compression wood has changed from one side of the stem to the other. This behaviour is considered typical of the righting mechanism of a tree. If such a study is repeated better notes need to be kept of the dimensions and shape of the sample.

Wood Properties – Shrinkage and Microfibril Angle

Warp (bow, crook, twist) is caused by differential shrinkage in the longitudinal, radial and tangential directions when water is removed from the wood cells. Longitudinal shrinkage increases with increasing microfibril angle, whereas tangential shrinkage decreases with increasing microfibril angle (Persson, 2000).

Data available

Longitudinal and tangential shrinkage were measured in 4 right-angled directions on one disc from 4 of the 5 bent trees (see SGMC Report No. 126 for measurement technique). There were 24 – 30 samples per disc giving a total of 111 samples. Strips, cut immediately below the shrinkage samples were processed through SilviScan, Group 3 of SilviScan data discussed above.

Longitudinal shrinkage was calculated as:

$$S_L = (L_f - L_i) / L_i$$

Tangential shrinkage was calculated as:

$$S_T = (T_f - T_i) / T_i$$

where:

S_L is the shrinkage in the longitudinal direction

S_T is the shrinkage in the tangential direction

L_i is the initial distance between the two pins

L_f is the final distance between the two pins

T_i is the initial width in the tangential direction

T_f is the final width in the tangential direction

Data analysis

The mean equilibrium moisture content for all samples, calculated after oven-drying, was 12.3%. The minimum and maximum values were 11.5% and 12.9% respectively.

Summary statistics for longitudinal and tangential shrinkage are shown in Table 11 and Table 12. The longitudinal shrinkage is much less than the tangential shrinkage, as has been observed previously e.g. (Gu *et al* 2001).

While there are only data from 4 trees, it is interesting to note that the mean longitudinal shrinkage was highest for tree 311 (from a high wood density clone). It would be worth confirming this result using more trees given the trend to increase tree density.

The shrinkage measurements and the SilviScan estimate of microfibril angle were compared, by making the assumption that the SilviScan ring boundaries and the shrinkage sample boundaries were equivalent.

The relationship between longitudinal shrinkage and microfibril angle is shown in Figure 8. The correlation between longitudinal shrinkage and microfibril angle was not significant ($p < 0.05$) for the four trees, either individually or combined. However it appears that longitudinal shrinkage for a given microfibril angle varies between the four trees, with tree C11 (311) having a higher longitudinal shrinkage for a given microfibril angle.

The relationship between tangential shrinkage and microfibril angle is shown in Figure 9. There was only a significant correlation between tangential shrinkage and microfibril angle for tree D09 (409). Trees D09 (409) and E22 (522) tended to have higher microfibril angles than the other 2 trees, but similar tangential shrinkage.

Table 11. Minimum, mean and maximum observed longitudinal shrinkage.

Seedlot	Unique No.	No. Obs.	Arithmetic Mean	Minimum	Maximum	Standard deviation
Long internode	224	30	0.00286	-0.000421	0.00576	0.00136
High wood density (GF18)	311	30	0.00378	0.00194	0.00697	0.00121
Low wood density (GF28)	409	24	0.00342	0.000582	0.00613	0.00126
Gwavas seed orchard (GF14)	522	27	0.00236	-0.000954	0.0105	0.00241

Note: These values are not percentages.

Table 12. Minimum, mean and maximum observed tangential shrinkage

Seedlot	Unique No.	No. Obs.	Arithmetic Mean	Minimum	Maximum	Standard deviation
Long internode	224	30	0.0367	0.0127	0.0952	0.0160
High wood density (GF18)	311	30	0.0342	0.00636	0.0827	0.0136
Low wood density (GF28)	409	24	0.0302	0.0117	0.0483	0.00877
Gwavas seed orchard (GF14)	522	27	0.0343	0.0192	0.0567	0.00996

Note: these values are not percentages.

Figure 8. Relationship between % longitudinal shrinkage and microfibril angle for four trees.

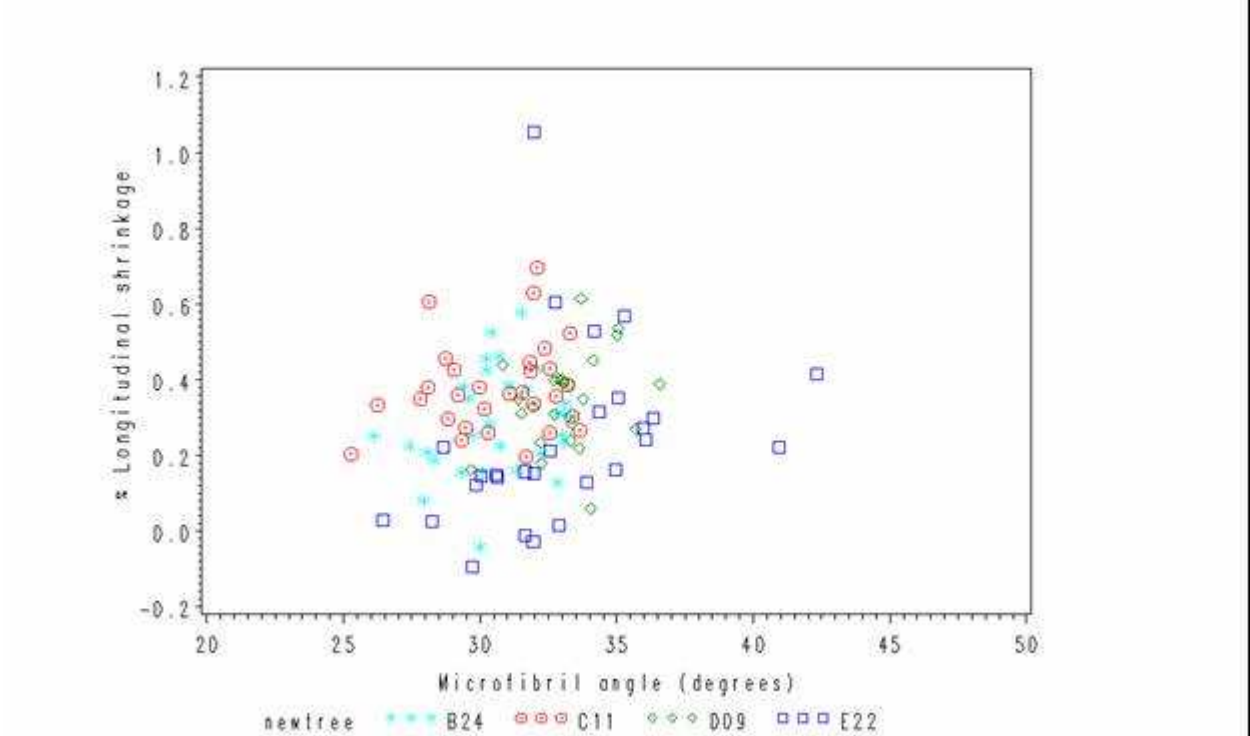
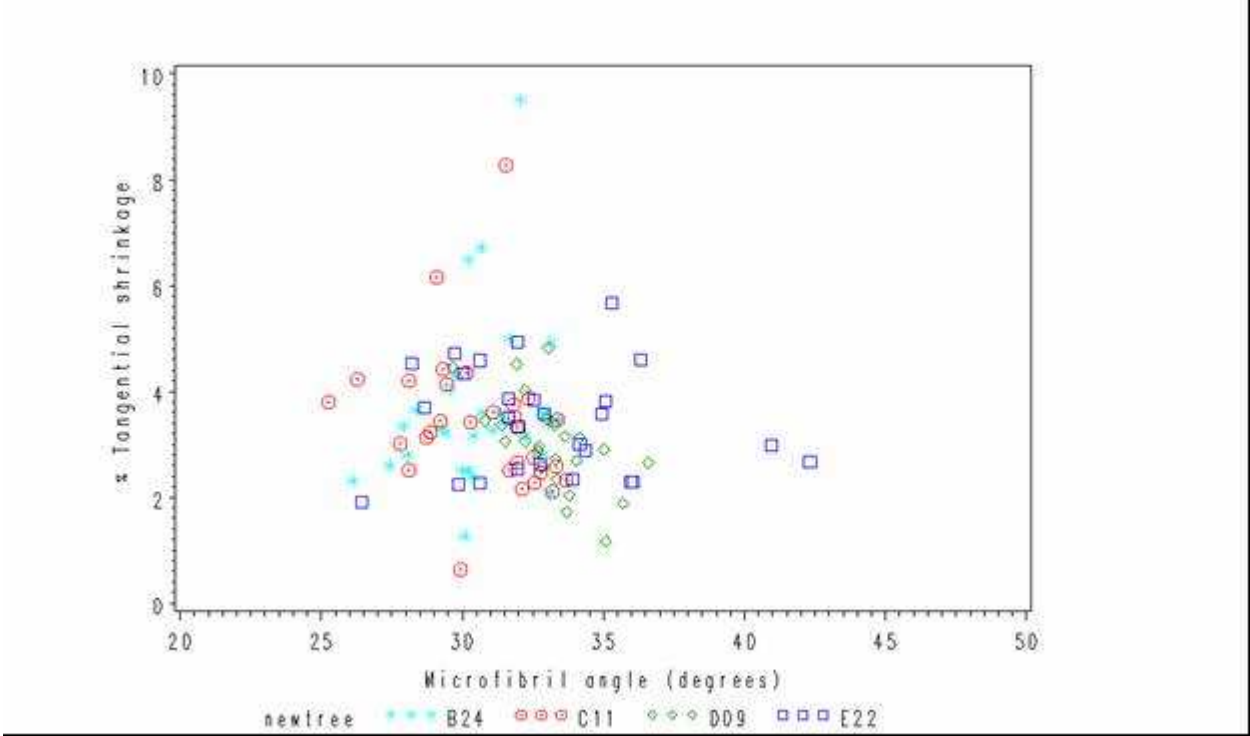


Figure 9. Relationship between % tangential shrinkage and microfibril angle for four trees.



Wood Properties – Branches

Burdon (1975) assessed compression wood in 18 radiata pine clones from each of 4 forest sites within New Zealand. He concluded that clones differed in their propensity to form compression wood. One way to determine a tree's ability to form compression wood would be to bend a tree over and allow it to right itself by forming compression wood in the stem. However compression wood is formed in branches. A hypothesis is that the variation in wood properties within a branch would indicate the tree's propensity to form compression wood.

Data available

SilviScan data (Group 6, discussed above) were obtained for 2 pith-bark strips from a number of branches. The branches were not selected in any systematic way. For some trees (the straight trees), the branch selected came from the cluster immediately above the internode sampled using SilviScan. The sample strips are shown in Appendix 6, Figure 13 and Figure 14.

Data analysis

The density profile for these branch strips were rather different from a stem density profile, in that the ring boundaries were not very obvious. For this reason the strip average values of wood properties have been analysed. For each branch, the differences in wood properties between the top and the bottom of the branch was calculated as:

strip average property for bottom strip minus strip average property for top strip

These differences were plotted against branch diameter and labelled by "Plot" (Figure 10, Figure 11, and Figure 12).

Insufficient branches were sampled to draw any firm conclusions, but there are indications that branch diameter and seedlot may influence the difference in wood properties between the base and the top of the branch. It is suggested that this hypothesis be pursued further. An unresolved question is whether we should be selecting branches of a specific diameter in relation to the tree DBH.

Figure 10. Difference in average density between base and top of selected branches.

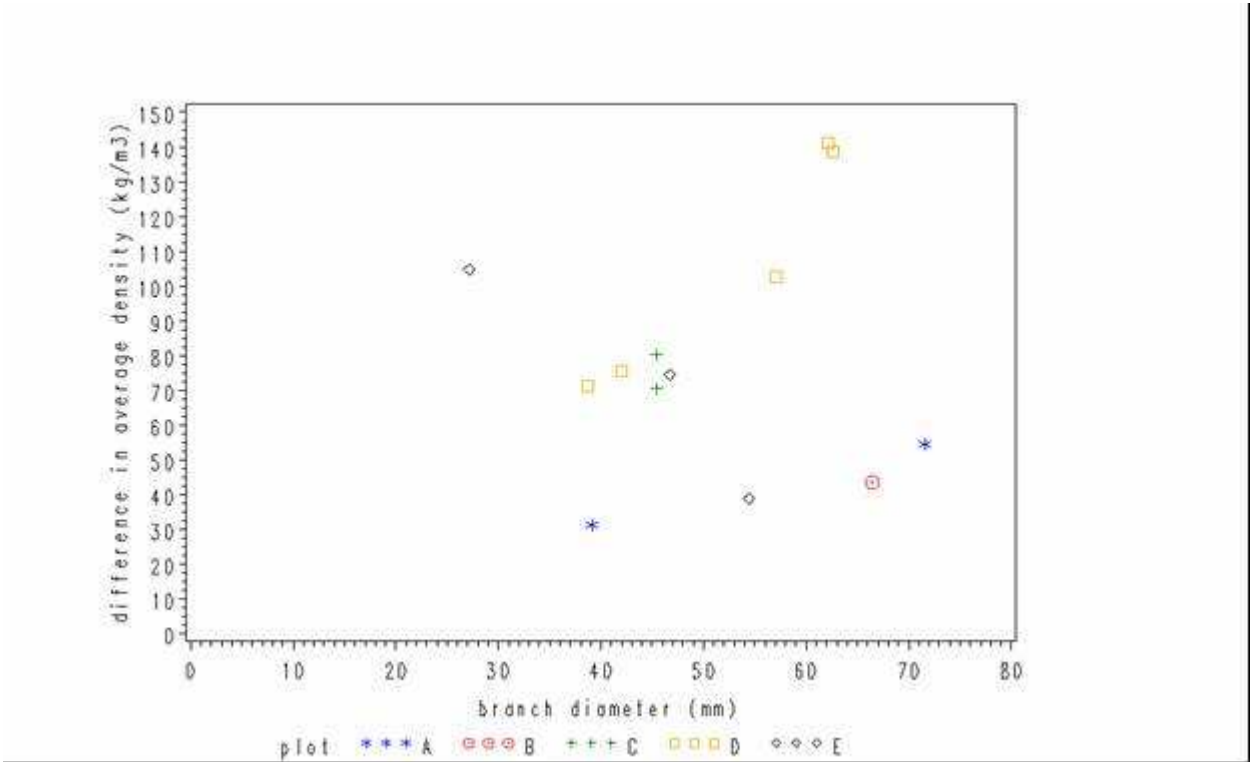


Figure 11. Difference in average MFA between base and top of selected branches.

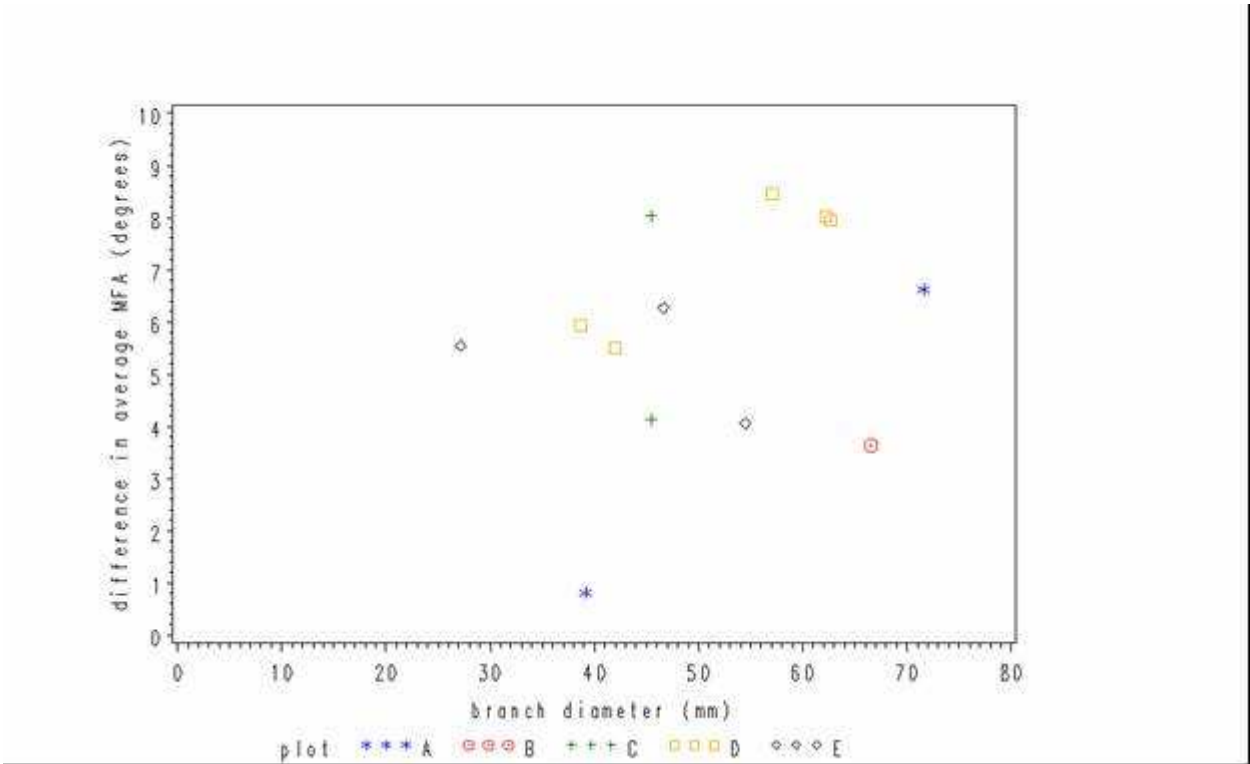
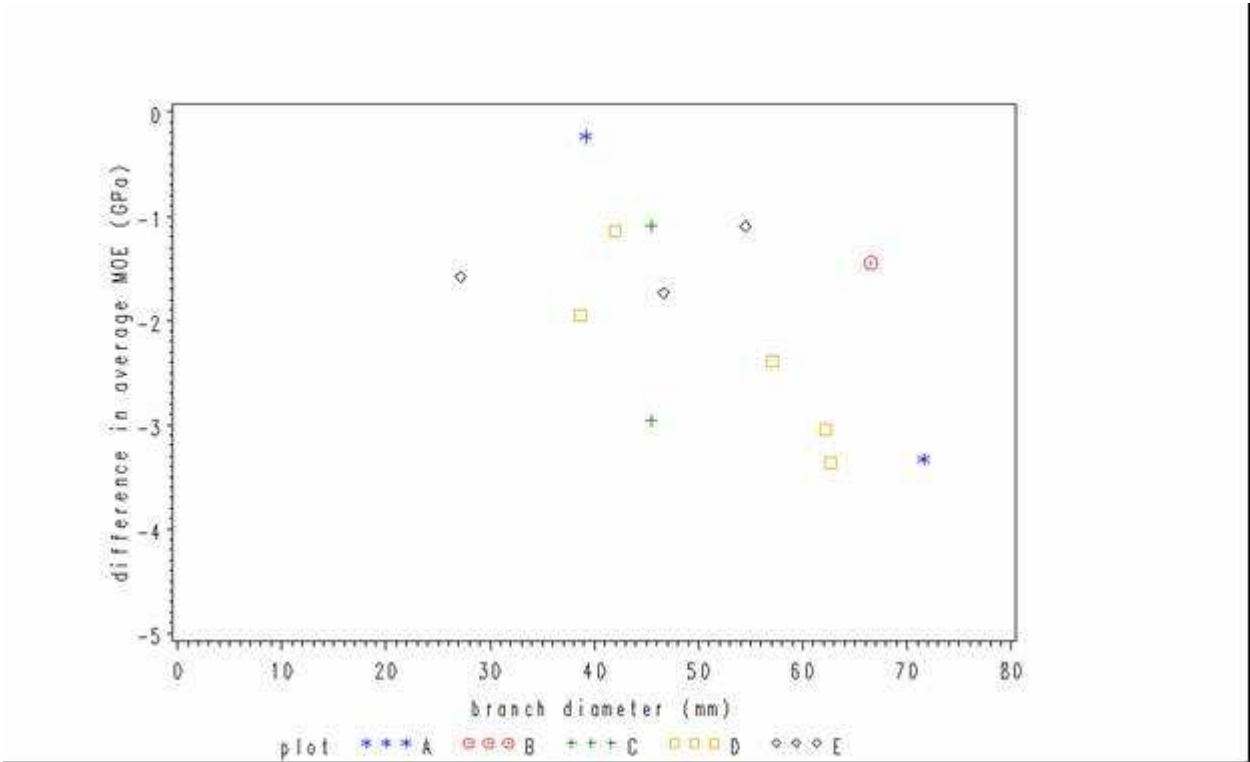


Figure 12. Difference in average MOE between base and top of selected branches.



Wood properties – relationship between branch and stem wood properties

One of the objectives of this study was to investigate whether the variation in wood properties between the upper and lower side of a branch were in any way related to the variation in stem wood properties due to the presence of compression wood.

Data Analysis

In this analysis, the SilviScan data from the internodes have been compared with the SilviScan data from the branch in the cluster immediately above the internode. For each branch the difference in a wood property was calculated as:

Strip average for base of branch minus strip average property for the top of the branch

For each internode, the absolute difference in strip average wood property was calculated for each level within the internode. The mean and maximum differences for the internode were then calculated.

The differences in wood properties within the internode were then compared with the differences in wood properties within the branch (Table 13). While none of the relationships were statistically significant ($p < 0.05$), there are some definite trends, indicating that it is worth pursuing the idea that the differences in branch wood properties can be used to tell us something about the variation, or potential, in stem wood properties.

Table 13. Comparison of stem wood properties with branch wood properties.

Mean difference between strip average wood properties at different levels within an internode	Maximum difference between strip average wood properties at different levels within an internode
Density	
<p>mean difference between pairs of strips</p> <p>difference in stem average density (kg/m³)</p> <p>difference in branch average density (kg/m³)</p> <p>tree: * A16, ○ A24, ++ C09, □ D11, ○ D13, △ E16, ■ E17</p>	<p>max difference between pairs of strips</p> <p>difference in stem average density (kg/m³)</p> <p>difference in branch average density (kg/m³)</p> <p>tree: * A16, ○ A24, ++ C09, □ D11, ○ D13, △ E16, ■ E17</p>
Microfibril angle	
<p>mean difference between pairs of strips</p> <p>difference in stem average MFA (degrees)</p> <p>difference in branch average MFA (degrees)</p> <p>tree: * A16, ○ A24, ++ C09, □ D11, ○ D13, △ E16, ■ E17</p>	<p>max difference between pairs of strips</p> <p>difference in stem average MFA (degrees)</p> <p>difference in branch average MFA (degrees)</p> <p>tree: * A16, ○ A24, ++ C09, □ D11, ○ D13, △ E16, ■ E17</p>
Longitudinal modulus of elasticity	
<p>mean difference between pairs of strips</p> <p>difference in stem average MOE (GPa)</p> <p>difference in branch average MOE (GPa)</p> <p>tree: * A16, ○ A24, ++ C09, □ D11, ○ D13, △ E16, ■ E17</p>	<p>max difference between pairs of strips</p> <p>difference in stem average MOE (GPa)</p> <p>difference in branch average MOE (GPa)</p> <p>tree: * A16, ○ A24, ++ C09, □ D11, ○ D13, △ E16, ■ E17</p>

Discussion and Recommendations

The objective of this study was to develop a procedure for destructive sampling tree growth, crown development and wood properties for use in rotation age trials.

With regards to the development of a practical field procedure the following points were noted:

- PhotoMARVL images should be taken of all sample trees, to be able to confirm standing stem form.
- Selection of sample branches for foliage measurement should be based on position in crown, rather than botanical age, because it is time-consuming to age branches based on botanical features.
- Samples to be saved for wood property measurements should be cut as discs, and be as thin as practical to reduce weight of material to be moved.
- Images should be taken of all samples saved for wood property measurement.
- Measurement of wood property variation within a disc is important to determine which trees with have highly variable wood properties.

The small number of trees sampled and the wide variability in the observed data made it difficult to draw any firm conclusions.

In terms of crown structure:

- The least square mean values for the number of branch clusters in an annual shoot ranged from 3.1 (for the long-internode seedlot) to 4.6 for the highly multinodal seedlot.
- The number of branches in a cluster was similar for all trees.

In terms of wood properties:

- Least square mean values of wood properties for the individual straight trees were not significantly correlated with tree DBH, but there were only a small number of trees from a wide range of seedlots.
- Tree 116 stood out as having a high density for its DBH.
- Based on these data, it is suggested that between 6 and 10 trees be destructively sampled from an individual seedlot or treatment in future studies.
- The relationship between microfibril angle and shrinkage appears to vary between individual trees.
- Wood properties varied vertically and circumferentially within an internode in the straight trees, presumably due to the presence of compression wood. Compression wood tends to have higher density and microfibril angle than normal wood. For these trees there is an indication that one property may vary more than the other. The two trees from the low wood density seedlot exhibited the greatest variation in density, while trees A16, and C09 exhibited the greater variation in MFA and MOE. This may indicate that different trees employ different strategies for compression wood formation.
- The variation in branch wood properties was compared with the variation in internode wood properties for the straight trees. While the correlations were not significant ($p < 0.05$), there is sufficient pattern in the graphs (Table 13) to suggest it is worth pursuing this approach with a second study and a larger sample size.

One of the most important points learnt from this study was the value of having images of the wood to compare with wood property values. Changes in density, microfibril angle and longitudinal modulus of elasticity appeared to be related to visual compression wood. In this study we had images of the strips. While the images of the strips were useful, it would have been even better to have images of the whole disc to be able to see how visual compression wood varied throughout the disc.

As part of a government funded study, we now have developed tools for taking images of whole discs and mapping visual compression wood. Another study is in progress to determine the relationship between visual colour and SilviScan wood properties.

While the images indicated that wood properties appear to be related to visual compression wood, the important unanswered question is:

What were the underlying causes that made these trees form the observed patterns of compression wood?

Two potential approaches to answer this question are:

- Carry out tree bending and tree flexing studies using different clones within a greenhouse. This would eliminate environmental effects.
- Monitor tree movement and stem form for a number of nominally straight trees in the field over 1 or 2 growing seasons and determine whether the distribution of compression wood is related to stem form or tree movement. A potential problem with this approach is how to monitor movement in the field.

It is considered that the first approach would give the better results. The project would be suitable as Ph.D. study for a student.

The other question that needs to be addressed is:

- How much do the observed variations in wood properties influence the behaviour of wood products?

References

Stand Growth Modelling Reports

114. Grace, J.C. 2003. Linking tree growth to end-product performance: Literature review and proposed modelling strategy.
126. Grace, J.C.; Andersen, C.; Hayes, J.D. 2005. Pilot study for internal stem modelling: Data Collection.

Other references

- Bannister, 1962: Some variation in the growth pattern of *Pinus radiata* in New Zealand. New Zealand Journal of Science 5: 342-370.
- Burdon, R.D. 1975: Compression wood in *Pinus radiata* clones on four different sites. New Zealand Journal of Forestry Science 5: 152-164.
- Harris, J.M. 1977: Shrinkage and density of radiata pine compression wood in relation to its anatomy and mode of formation. New Zealand Journal of Forestry Science 7(1): 91-106.
- Harris, J.M.; Cown, D.J. 1991: Basic wood properties. Chapter 6 In Kininmonth, J.A.; Whitehouse, L.J. (ed) Properties and uses of New Zealand radiata pine Vol. 1 – Wood properties. Ministry of Forestry, Forest Research Institute.
- Gu, H.; Zink-Sharp, A.; Sell, J. 2001: Hypothesis on the role of the cell wall structure in differential transverse shrinkage of wood. Holz als Roh- und Werkstoff 59: 436-442.
- Ormarsson, S. 1999: Numerical analysis of moisture-related distortions in sawn timber. Department of Structural Mechanics, Chalmers University of Technology, Göteborg, Sweden, Publication 99:7.
- Persson, K. 2000: Micromechanical modelling of wood and fibre properties. Doctoral Thesis, Department of Mechanics and Materials, Lund University, Lund, Sweden.
- Pont D. 2003. A model of secondary growth for radiata pine. M.F.Sc. thesis, University of Canterbury, Christchurch, 183pp.
- Skatter, S.; Archer, R.R. (unpublished): Within-stem growth stress distribution in the case of spiral grain.

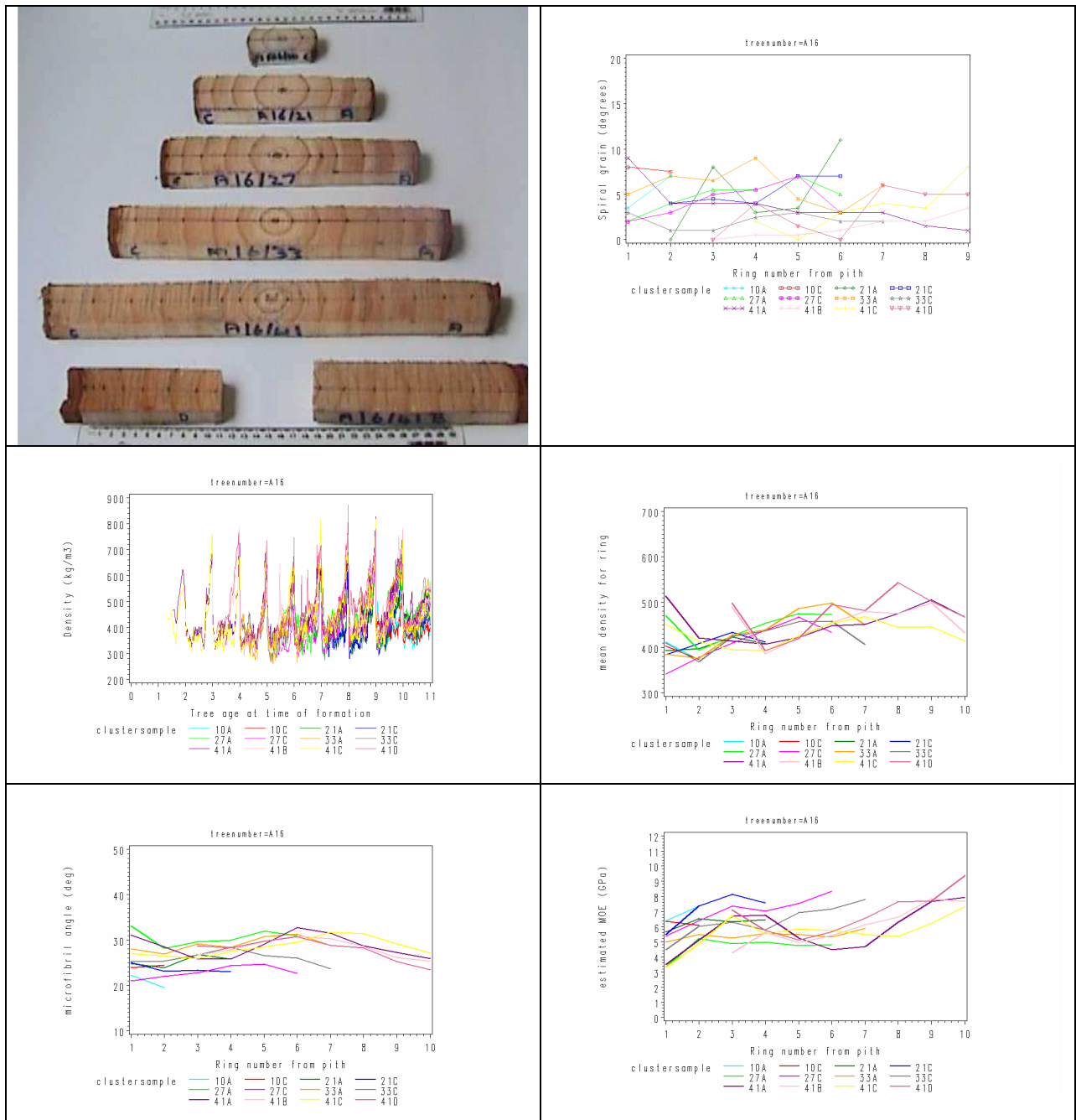
Appendix 1. Variation in stem wood properties for individual straight trees

The following tables are laid out as follows:

Table 14. Layout for tables of images in Appendix 1.

Image of wood samples	Spiral grain versus ring number from the pith, i.e. wood formed in one year may be at different horizontal positions within the graph.
SilviScan density profiles versus tree age at time of formation, i.e. all wood formed in one year is in the same horizontal position in the graph.	Ring average density (from SilviScan) versus ring number from the pith.
Ring average microfibril angle (from SilviScan) versus ring number from the pith	Ring average longitudinal modulus of elasticity (from SilviScan) versus ring number from the pith.

Table 15. Tree 116: Straight tree, highly multinodal family, DBH 388 mm



Notes

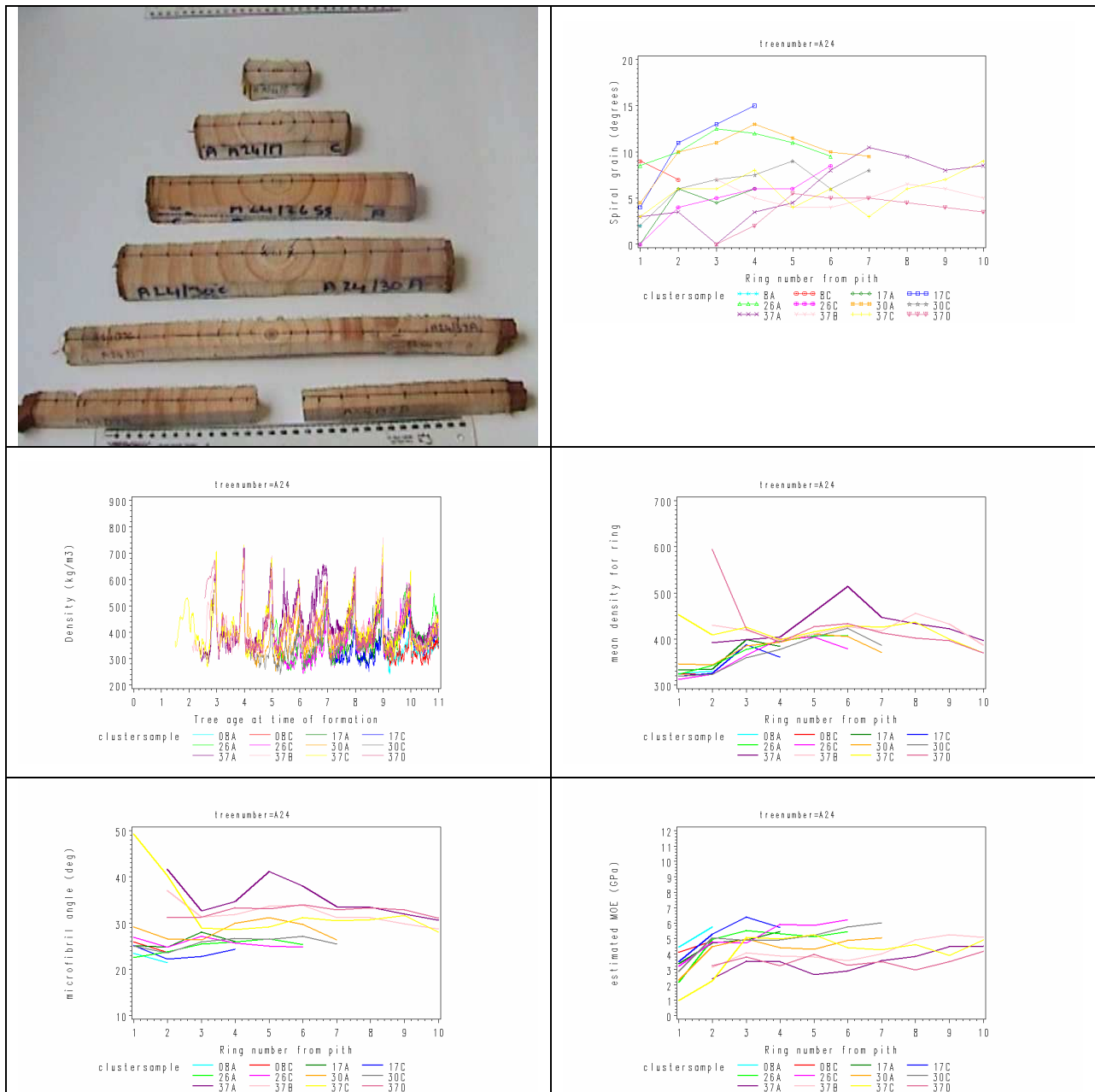
In the photograph: strip A16/41B is at the bottom right and strip A16/41D at the bottom left. Average values are shown for the measurements made on the incomplete innermost ring of the B and D strips.

Comments

Some rings in samples 27A and 41A appear to contain compression wood (visually darker colour).

- MFA tends to be higher in these rings.
- MOE tends to be lower in these rings.

Table 16. Tree 124: Straight tree, highly multinodal family, DBH 385 mm



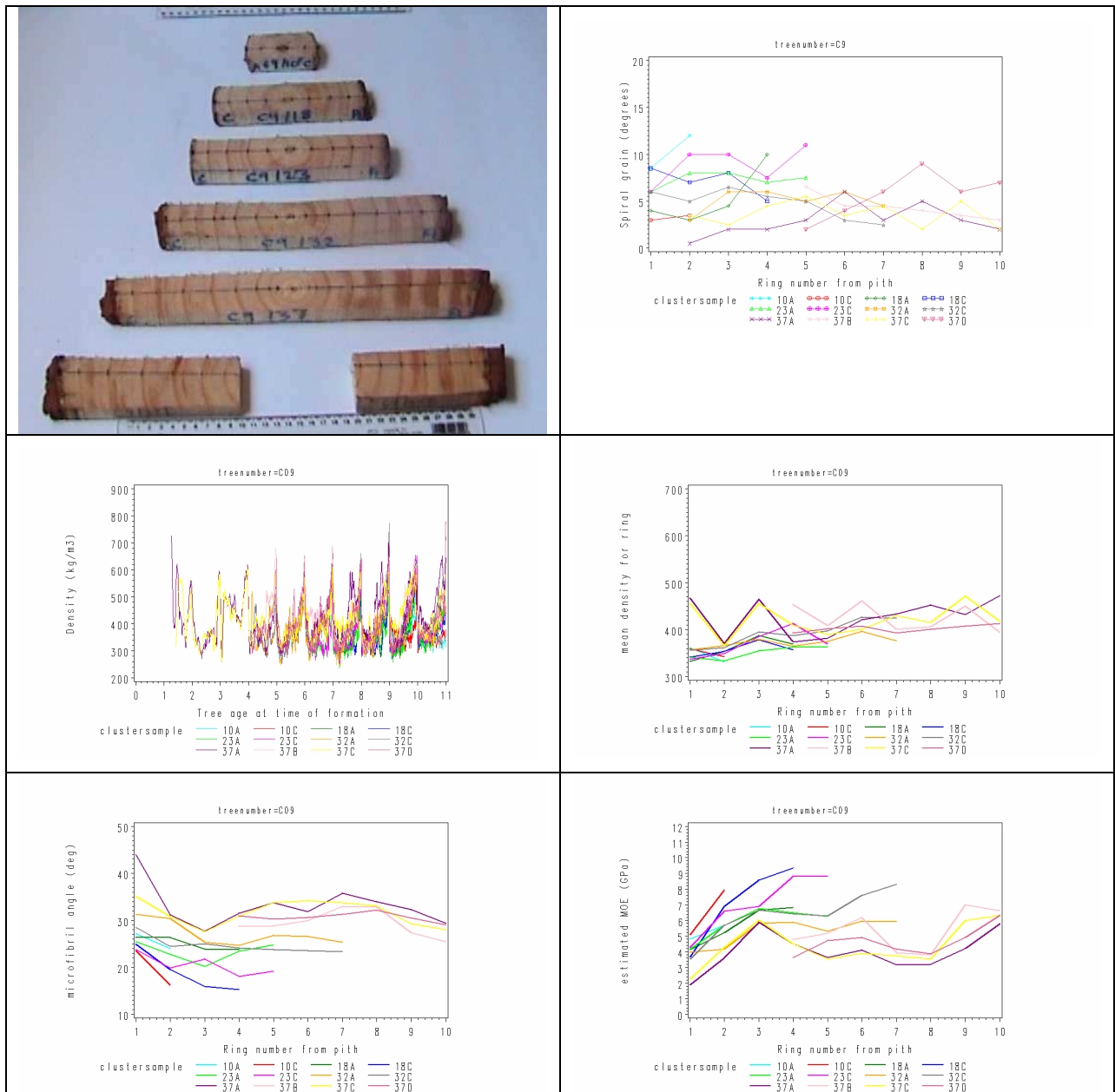
Notes

In the photograph: strip A24/37B is at the bottom left and strip A24/37D at the bottom right. Average values are shown for the measurements made on the incomplete innermost ring of the B and D strips.

Comments

Sample 37A stands out as having a few rings with compression wood. These rings tend to have higher density, higher MFA and lower MOE.

Table 17. Tree 309: Straight tree, high wood density family



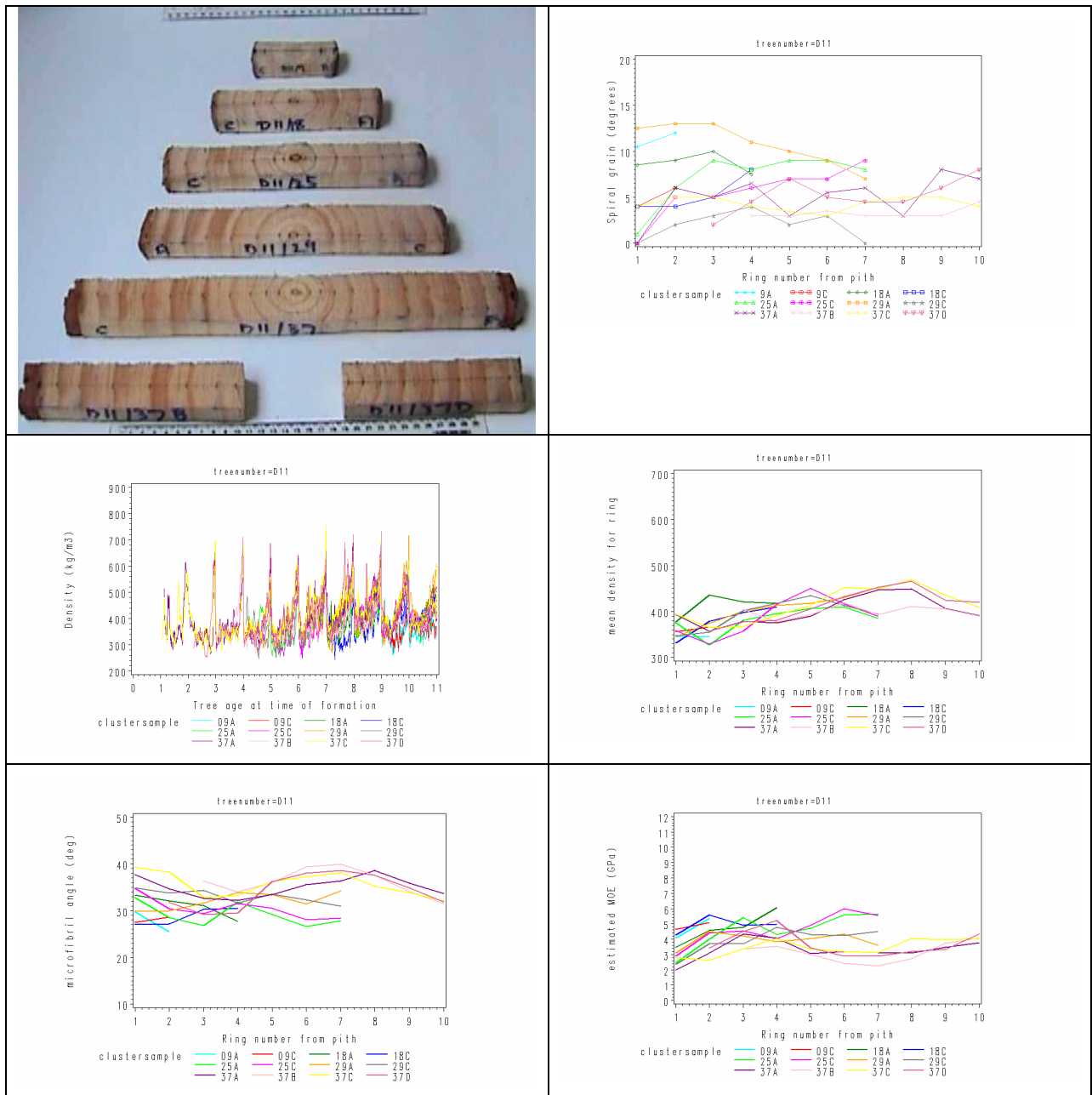
Notes

In the photograph: strip C09/37B is at the bottom right and strip C09/37D at the bottom left. Average values are shown for the measurements made on the incomplete innermost ring of the B and D strips.

Comments

Sample 37A stands out as having visual compression wood in some rings. Again these rings tend to have higher density, higher MFA and lower MOE.

Table 18. Tree 411, Straight tree, low wood density family



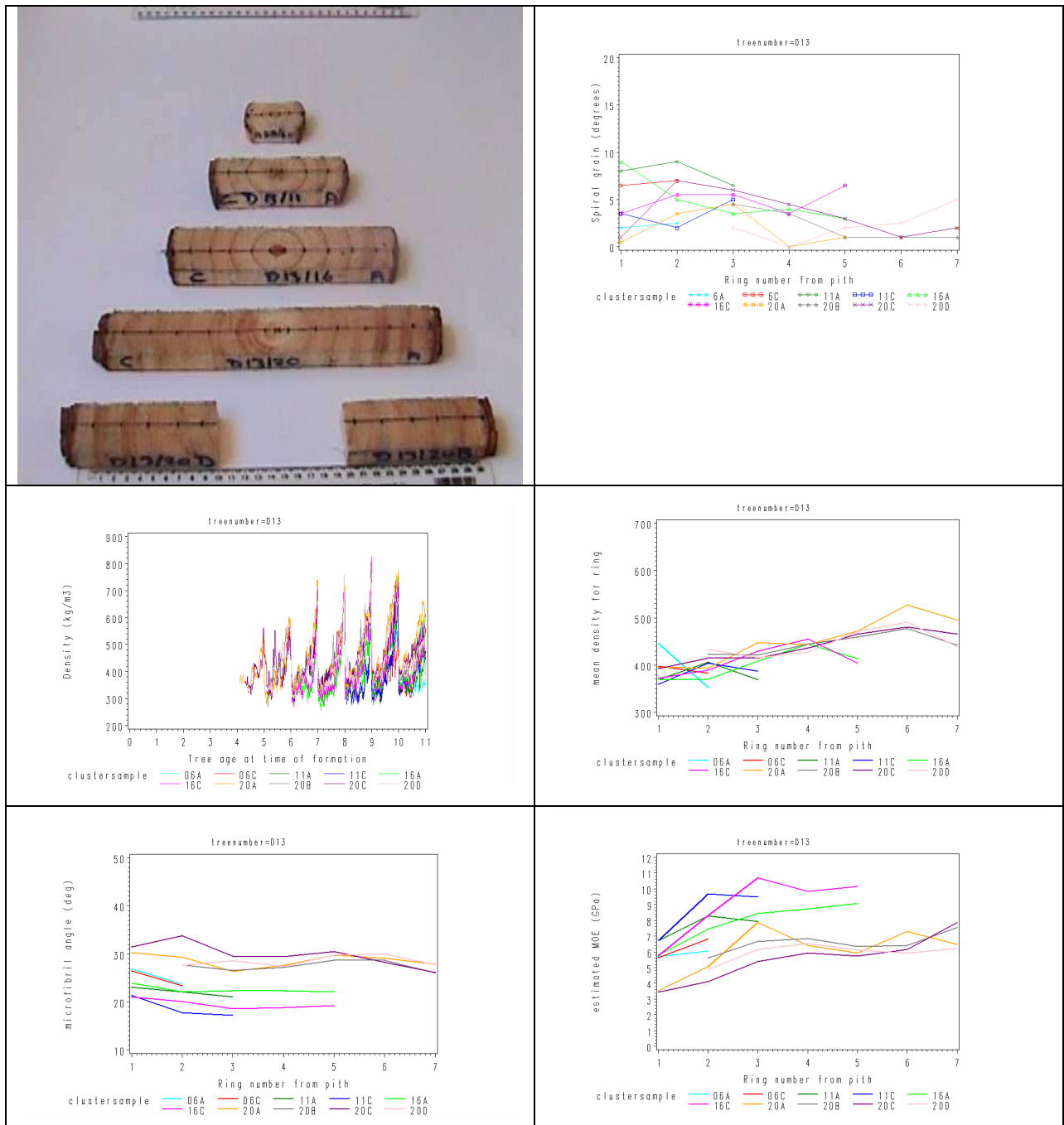
Note:

Average values are shown for the measurements made on the incomplete innermost ring of the B and D strips.

Comments

A number of samples appear to contain some compression wood. For level 37, MFA tends to be higher and MOE lower where there is visual compression wood.

Table 19. Tree 413, Straight tree, low wood density family



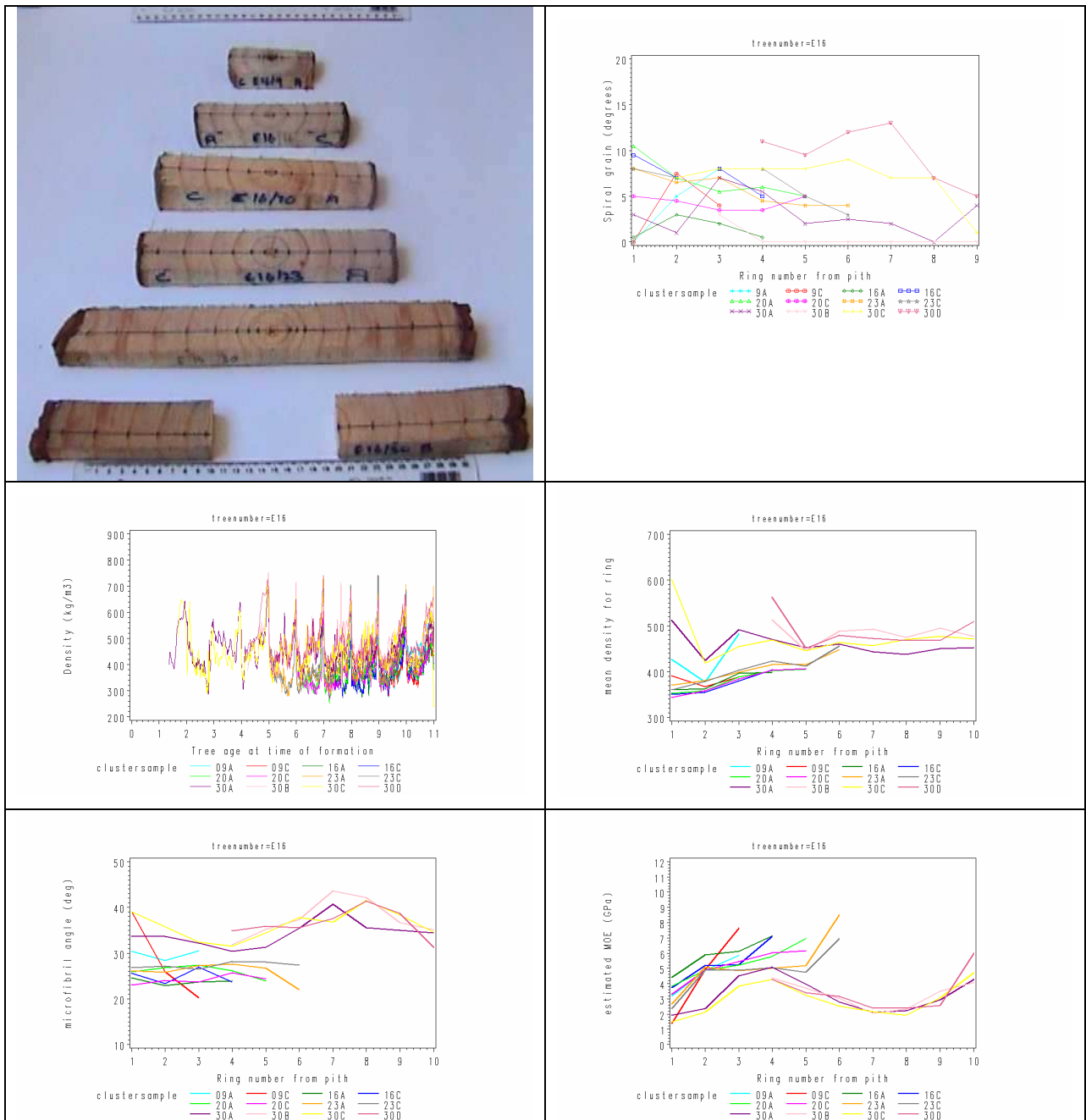
Notes

In the photograph: strip D13/20B is at the bottom right and strip D13/20D at the bottom left. Average values are shown for the measurements made on the incomplete innermost ring of the B and D strips.

Comments

These samples are quite interesting, in that there are only small patches of visual compression wood, but there is a lot of variation in MFA and MOE. The higher values of MFA and lower values of MOE tend to occur in the lowest disc.

Table 20. Tree 516, Straight tree from GF14



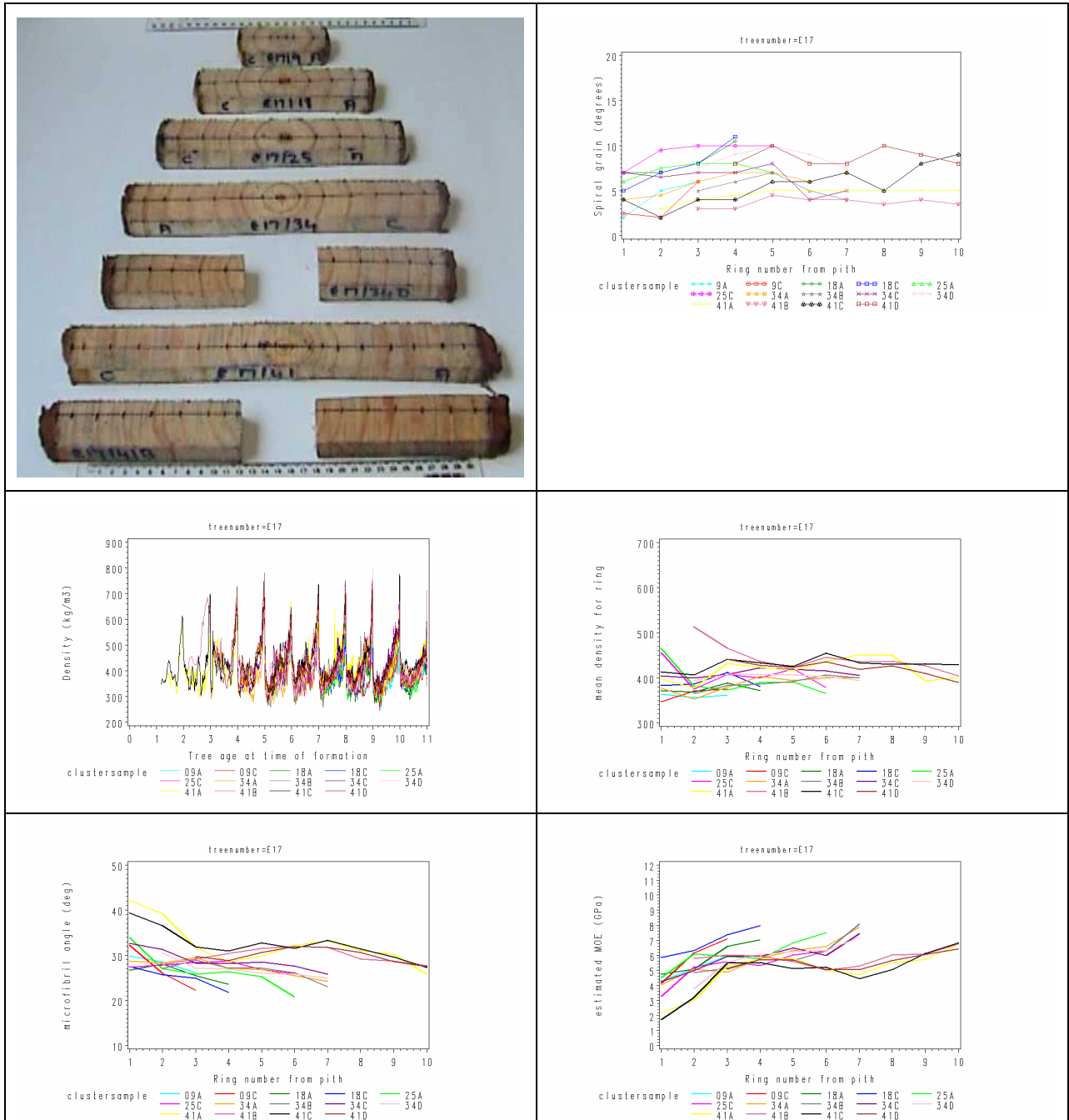
Notes

In the photograph: strip E16/30B is at the bottom right and strip E16/30D at the bottom left. Average values are shown for the measurements made on the incomplete innermost ring of the B and D strips.

Comments

The higher MFA and lower MOE values tend to be from the lowest disc. The increase in MFA and decrease in MOE around rings 6 to 9 is interesting. There appears to be visual compression wood in some of these rings.

Table 21. Tree 517, Straight tree from GF14



Notes

In the photograph: strip E17/41B is at the bottom left and strip E17/41D at the bottom right. Average values are shown for the measurements made on the incomplete innermost ring of the B and D strips.

Comments

There appears to be some visual compression wood in the samples from the lowest disc (41). MFA tends to be higher, and MOE tends to be lower in this disc.

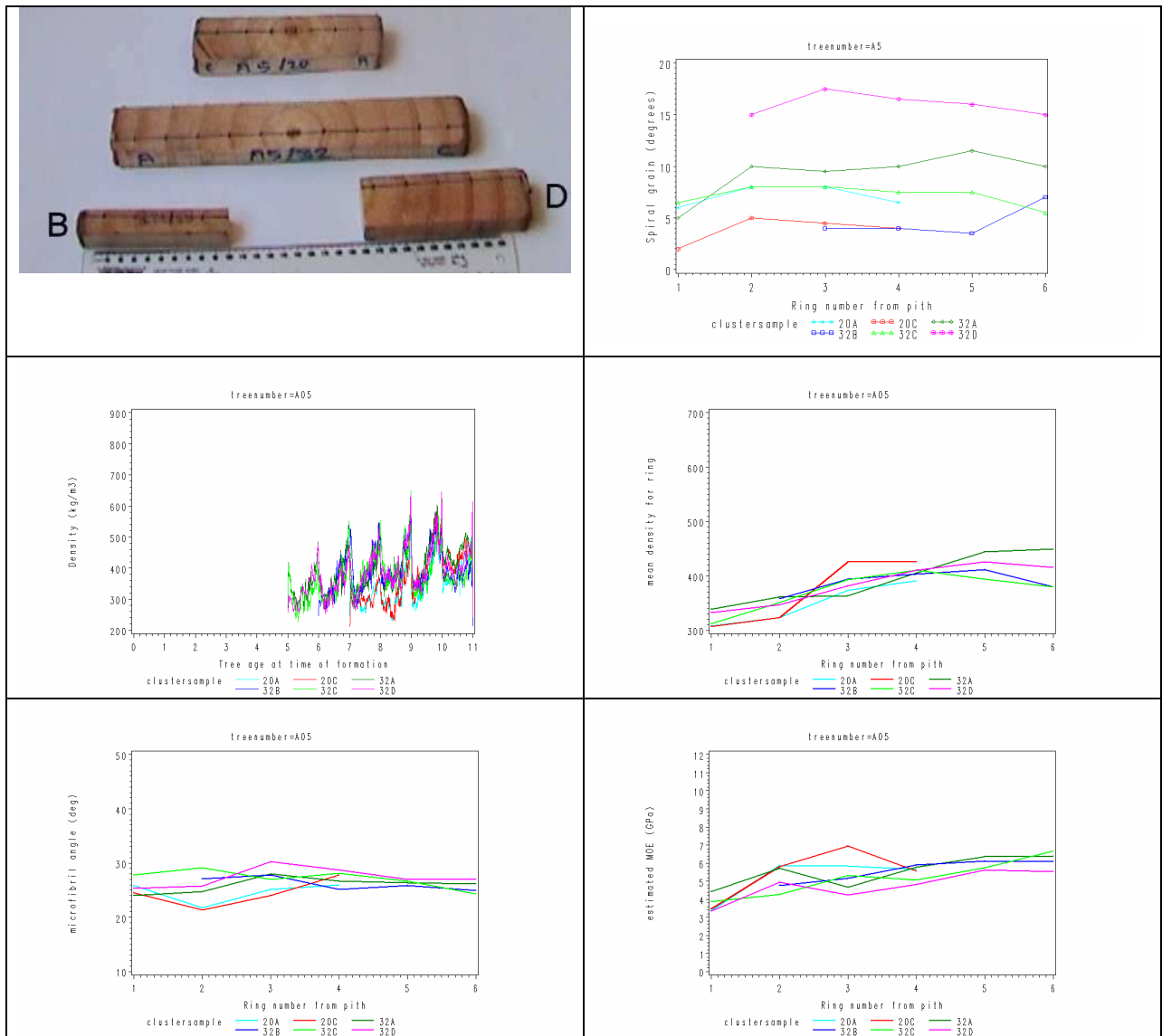
Appendix 2. Variation in stem wood properties for individual bent trees

The following tables are laid out as follows:

Table 22. Layout for tables of images in Appendix 2.

Image of wood samples	Spiral grain versus ring number from the pith, i.e. wood formed in one year may be at different horizontal positions within the graph.
SilviScan density profiles versus tree age at time of formation, i.e. all wood formed in one year is in the same horizontal position in the graph.	Ring average density (from SilviScan) versus ring number from the pith.
Ring average microfibril angle (from SilviScan) versus ring number from the pith	Ring average longitudinal modulus of elasticity (from SilviScan) versus ring number from the pith.

Table 23. Tree 105: Bent tree, highly multinodal family, DBH 381 mm



Note:

Average values are shown for the measurements made on the incomplete innermost ring of the B and D strips.

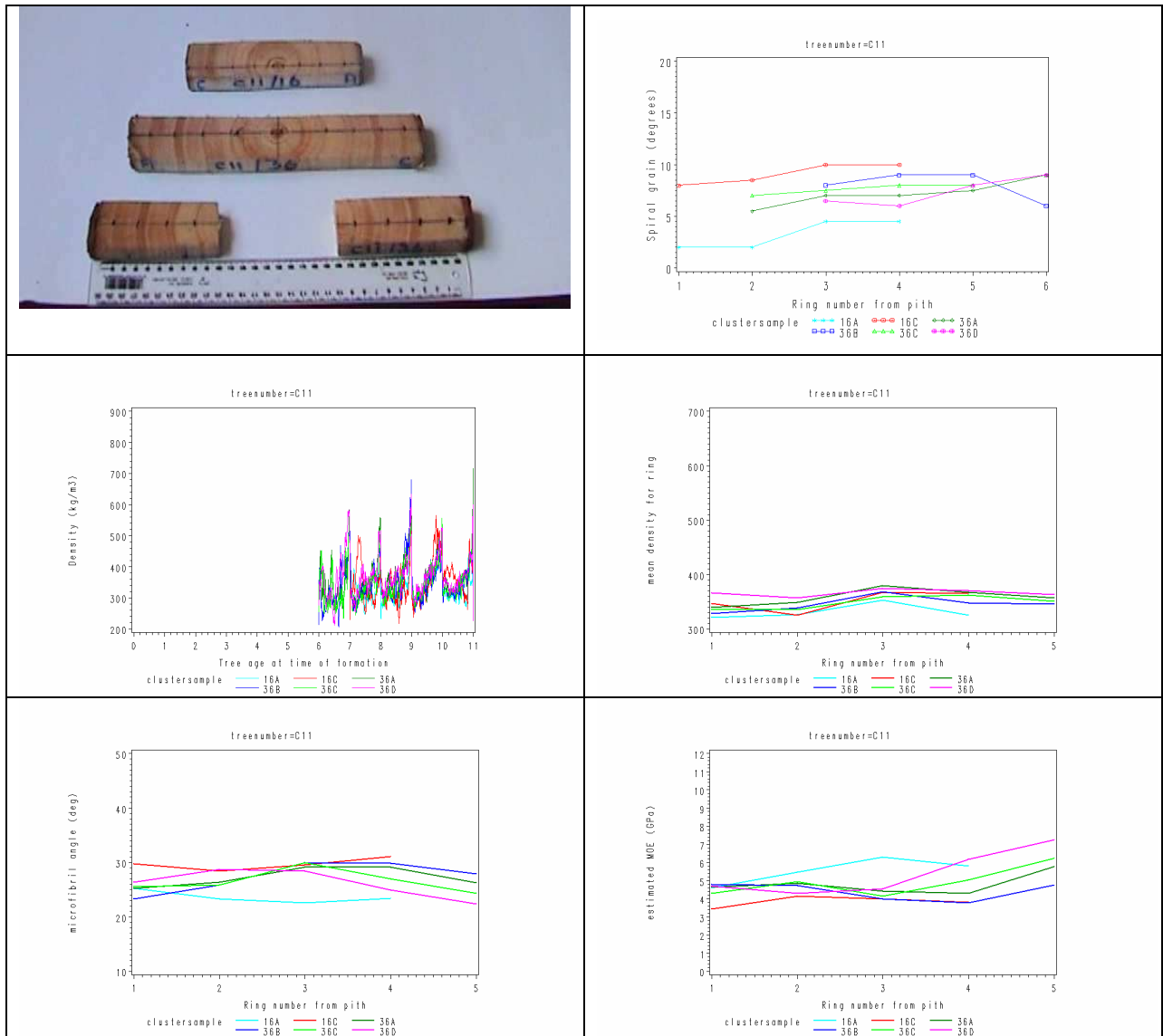
Comments:

Visually the samples from these trees appear to have a similar amount of compression wood to the samples from the straight trees from this seedlot.

Sample 32D appears to contain compression wood (visually the wood appears darker).

- It has the highest spiral grain of all samples
- MFA tends to be high compared with other samples
- MOE tends to be low compared to other samples

Table 24. Tree 311: Bent tree, high wood density family



Notes

In the Photograph strip C11/36B is on the left and strip C11/36D is on the right
 Average values are shown for the measurements made on the incomplete innermost ring of the B and D strips.
 Growth unit 36 contained 9 growth rings. Therefore the samples labelled 36 are incorrectly labelled. It is considered that they were from growth unit 26.

Comments

Visually, these samples appear to have a similar amount of compression wood to the straight tree from this seedlot (tree 309).

A number of rings appear to contain a little compression wood. Samples 16A and 16C stand out as being the most different. Sample 16C contains compression wood, has higher spiral grain, higher MFA and lower MOE. Sample 16A has no obvious compression wood, lower spiral grain, lower MFA and higher MOE.

Appendix 3. Wood Property variation within an internode

Comments

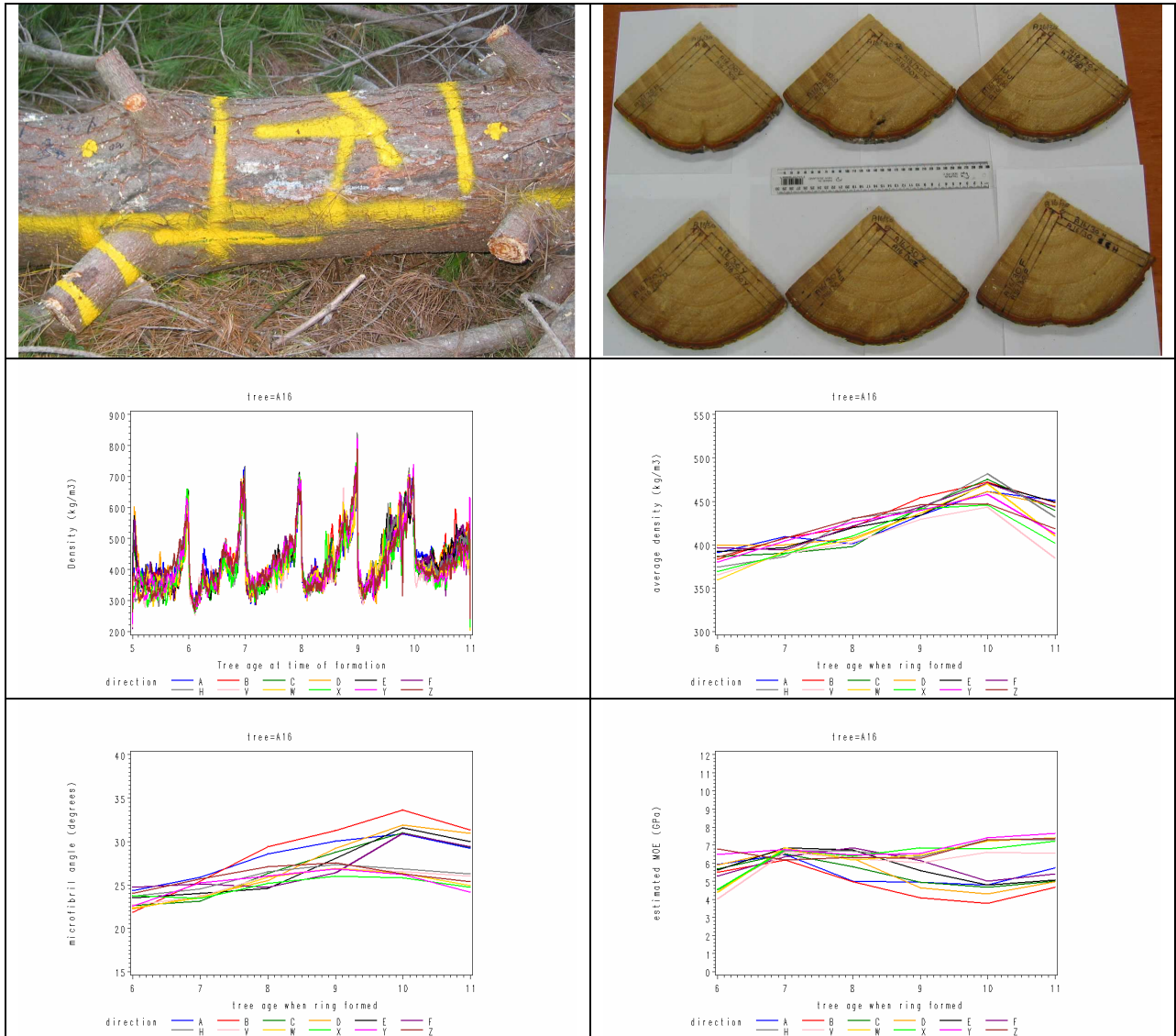
Wedges were cut from internodes in order to avoid carrying the whole internode from the forest. This only gave a limited picture of the circumferential variation in wood properties.

The following tables are laid out as follows:

Table 25. Layout for tables of images in Appendix 3.

Image of the internode before it was removed from the tree.	Images of the SilviScan samples before they were cut from the wedges.
SilviScan density profiles versus tree age at time of formation, i.e. all wood formed in one year is in the same horizontal position in the graph.	Ring average density (from SilviScan) versus tree age when the ring was formed.
Ring average microfibril angle (from SilviScan) versus tree age when the ring was formed.	Ring average longitudinal modulus of elasticity (from SilviScan) versus tree age when the ring was formed.

Table 26. Internode from tree A16



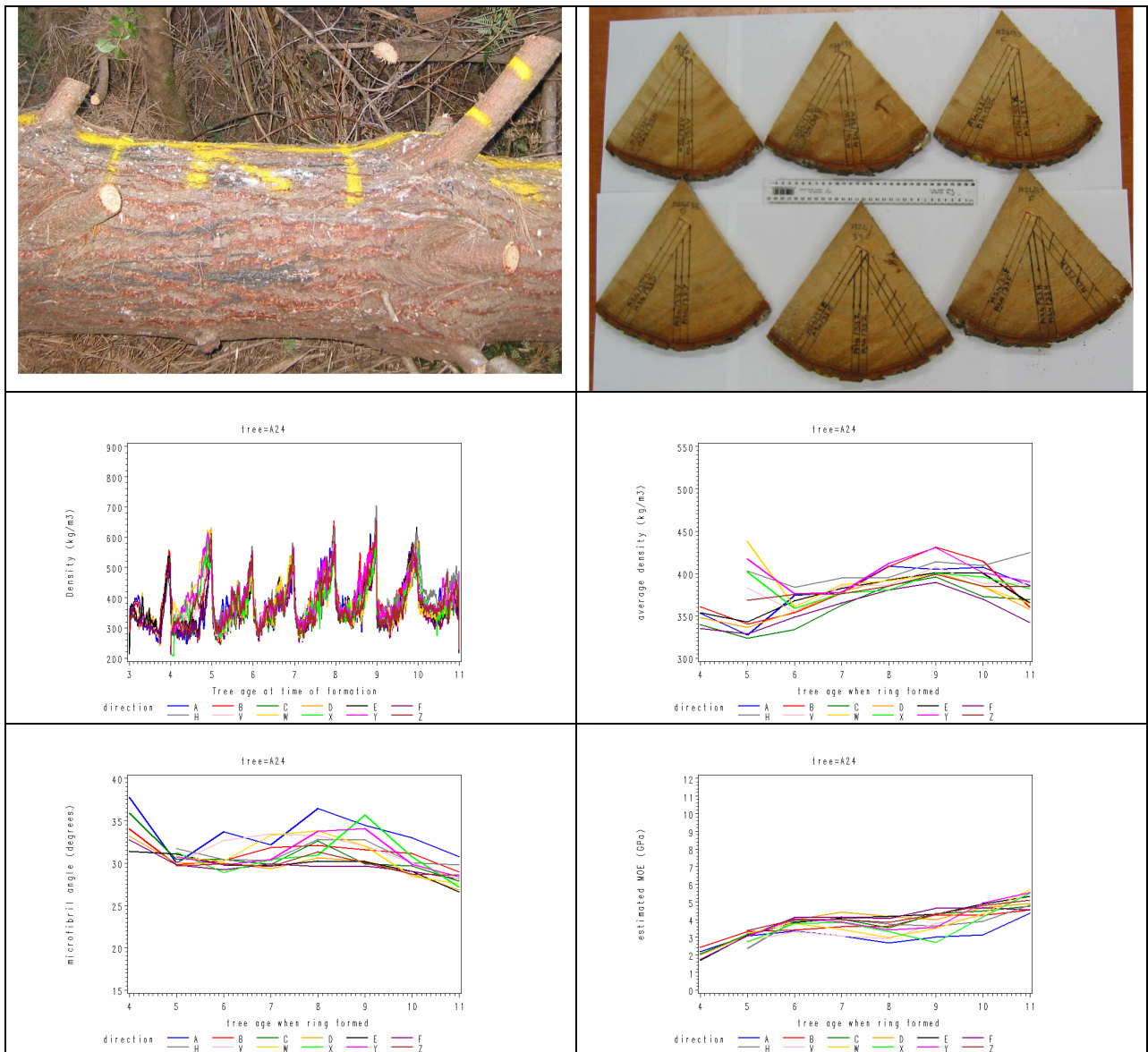
Note

The innermost ring on each sample may not be complete, and hence averages for that ring should be treated with caution.

Comments

There is little difference in visual colour between the different wedges. The outer two –three rings on the left-hand side of each wedge appear to be darker (visual compression wood). These samples have slightly higher density, higher MFA and lower MOE compared to the samples on the right hand side.

Table 27. Internode from tree A24



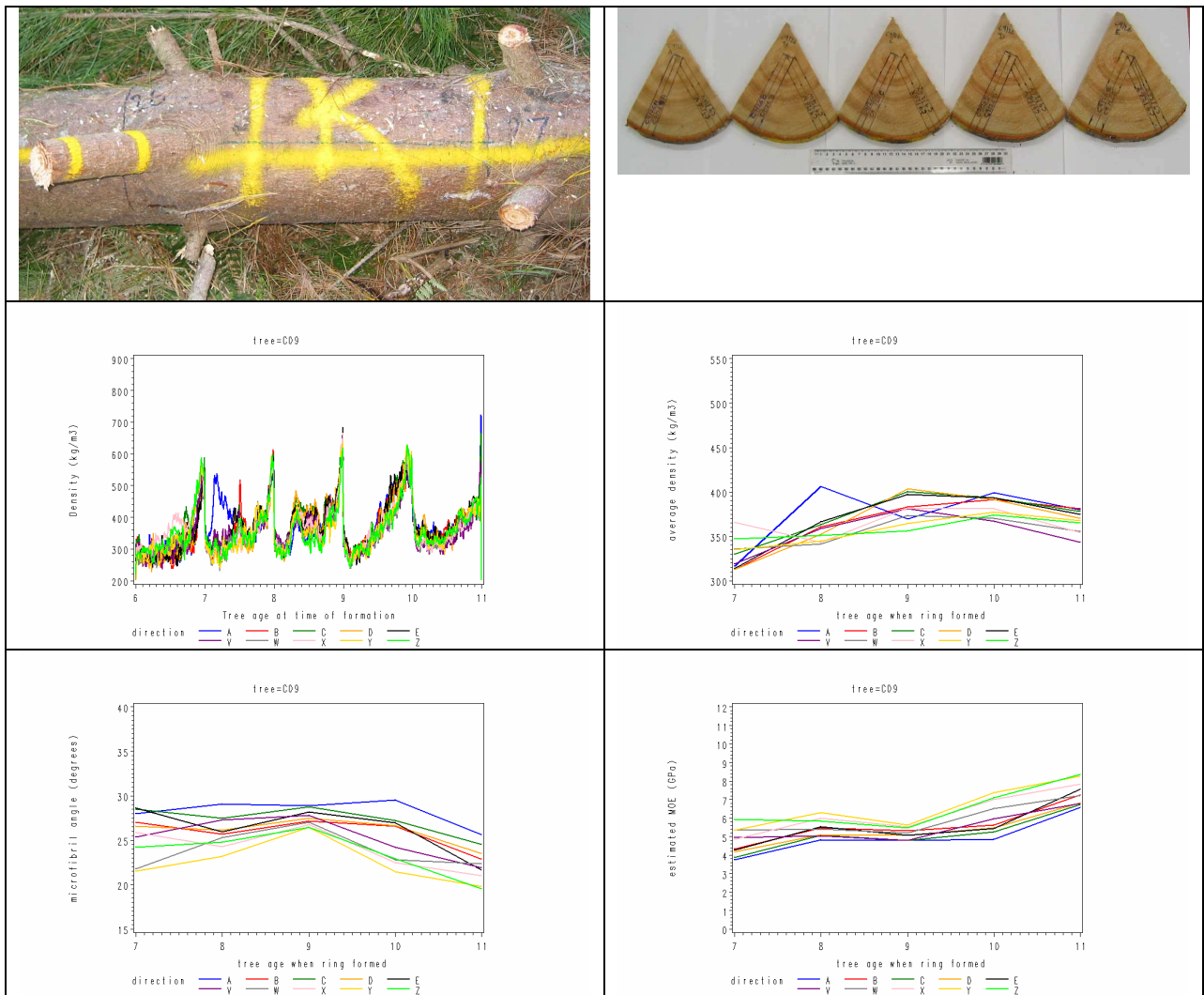
Note

The innermost ring on each sample may not be complete, and hence averages for that ring should be treated with caution.

Comments

There was patchy visual compression wood in some of these wedges. Direction A stands out as having higher MFA and lower MOE. It is possibly slightly darker than some of the other samples. This direction was nearest the branch cluster and under the sample branch. The differences between different strips are not as distinct as for tree A16.

Table 28. Internode from tree C09



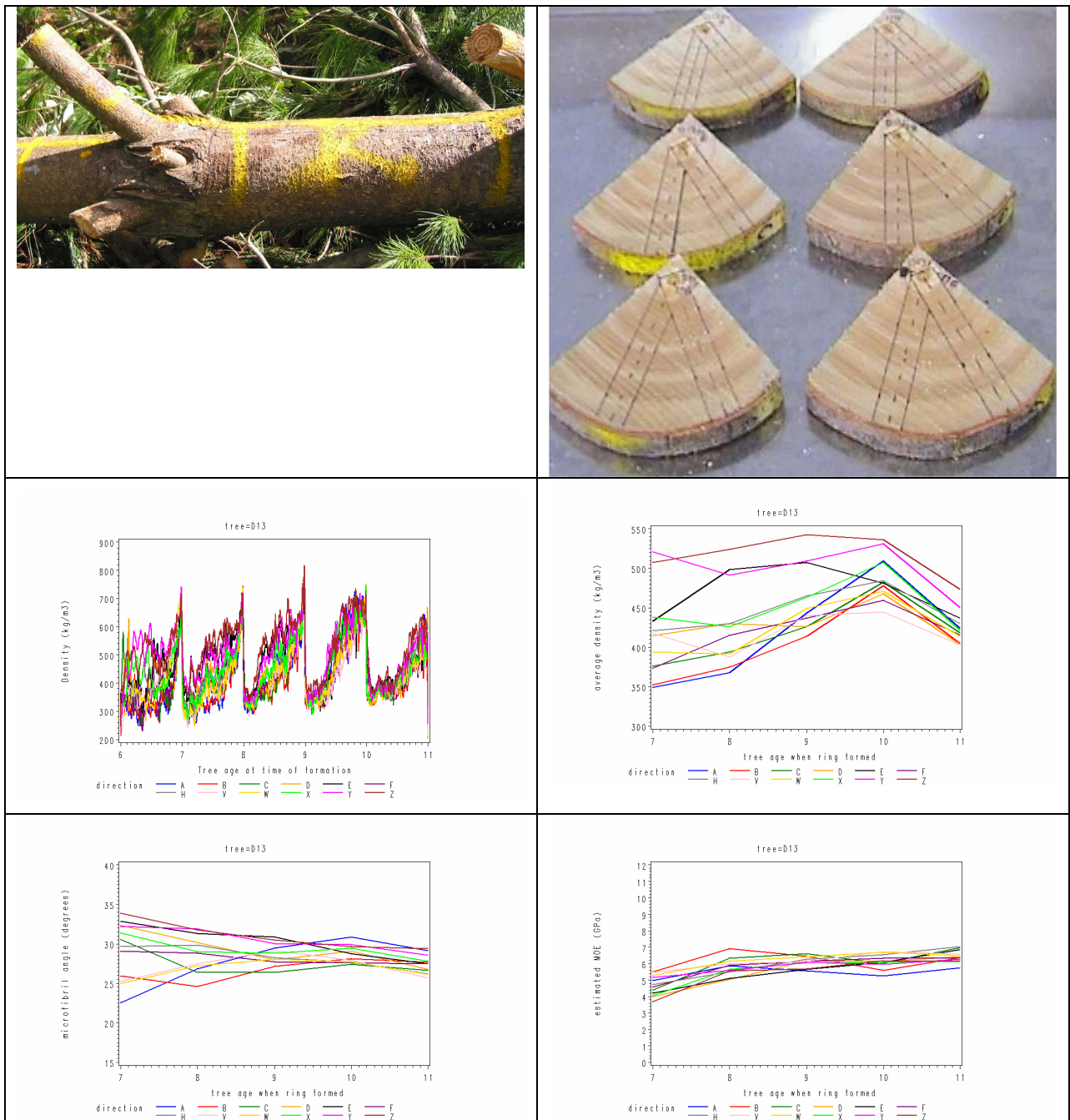
Note

The innermost ring on each sample may not be complete, and hence averages for that ring should be treated with caution.

Comments

There was patchy visual compression wood throughout these wedges. Directions A and C stand out as having higher MFA and lower MOE. These are the directions that were nearest to the branch cluster and under the sample branch. For direction A, the trace of density formed between ages 6 and 7 was noticeably higher than for other samples. The colour is possibly darker than in other wedges.

Table 29. Internode from tree D13



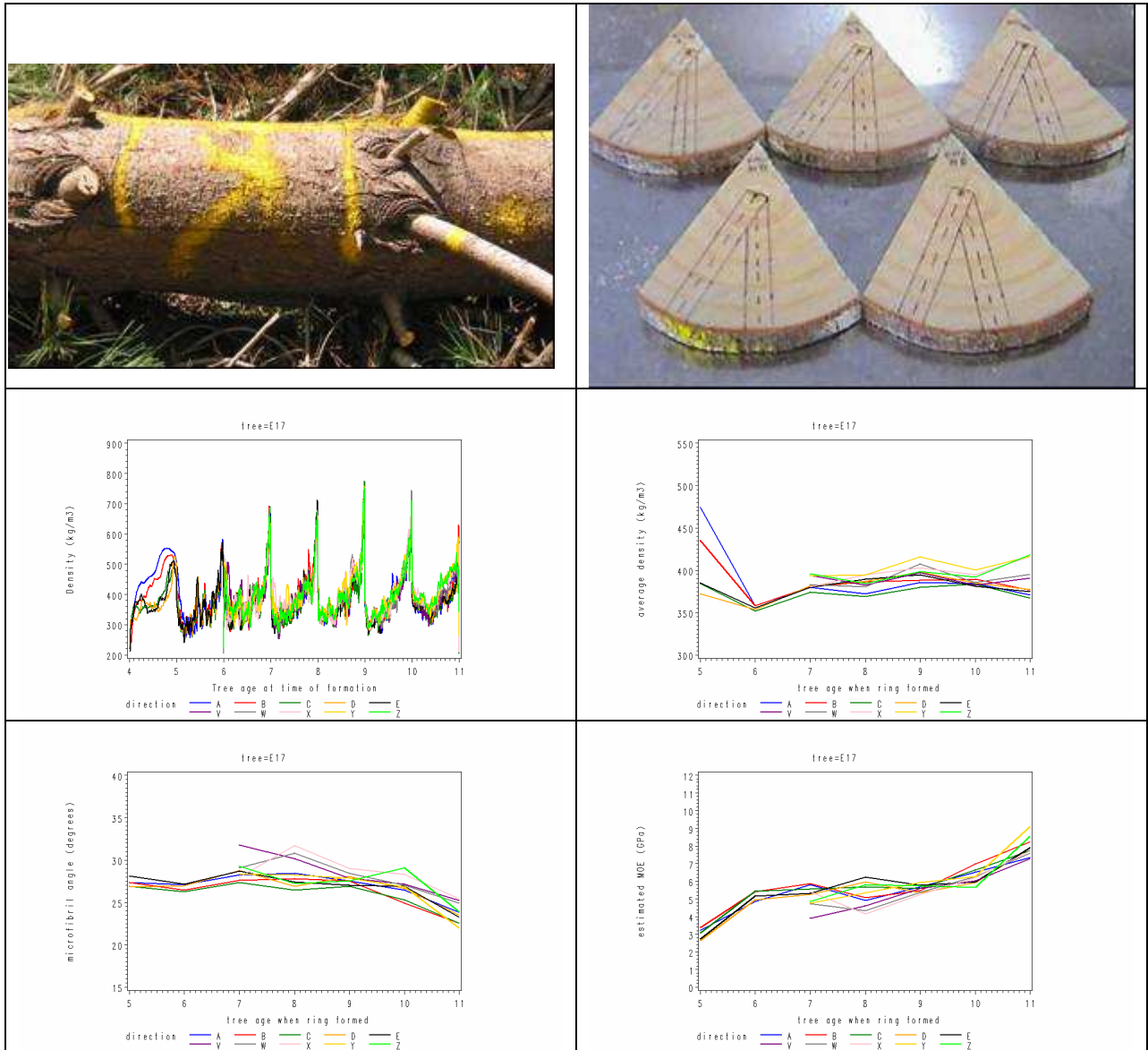
Note

The innermost ring on each sample may not be complete, and hence averages for that ring should be treated with caution.

Comments

These samples are quite interesting in that they all look a similar colour and appear to have a lot of compression wood. However there are wide variations in density between the different directions. It is also worth noting that the MOE for the different directions are very similar.

Table 30. Internode from tree E17



Note

The innermost ring on each sample may not be complete, and hence averages for that ring should be treated with caution.

Comments

None of these samples appeared to have much visual compression wood. There was little variation in density, MFA and MOE between the different directions at a given age.

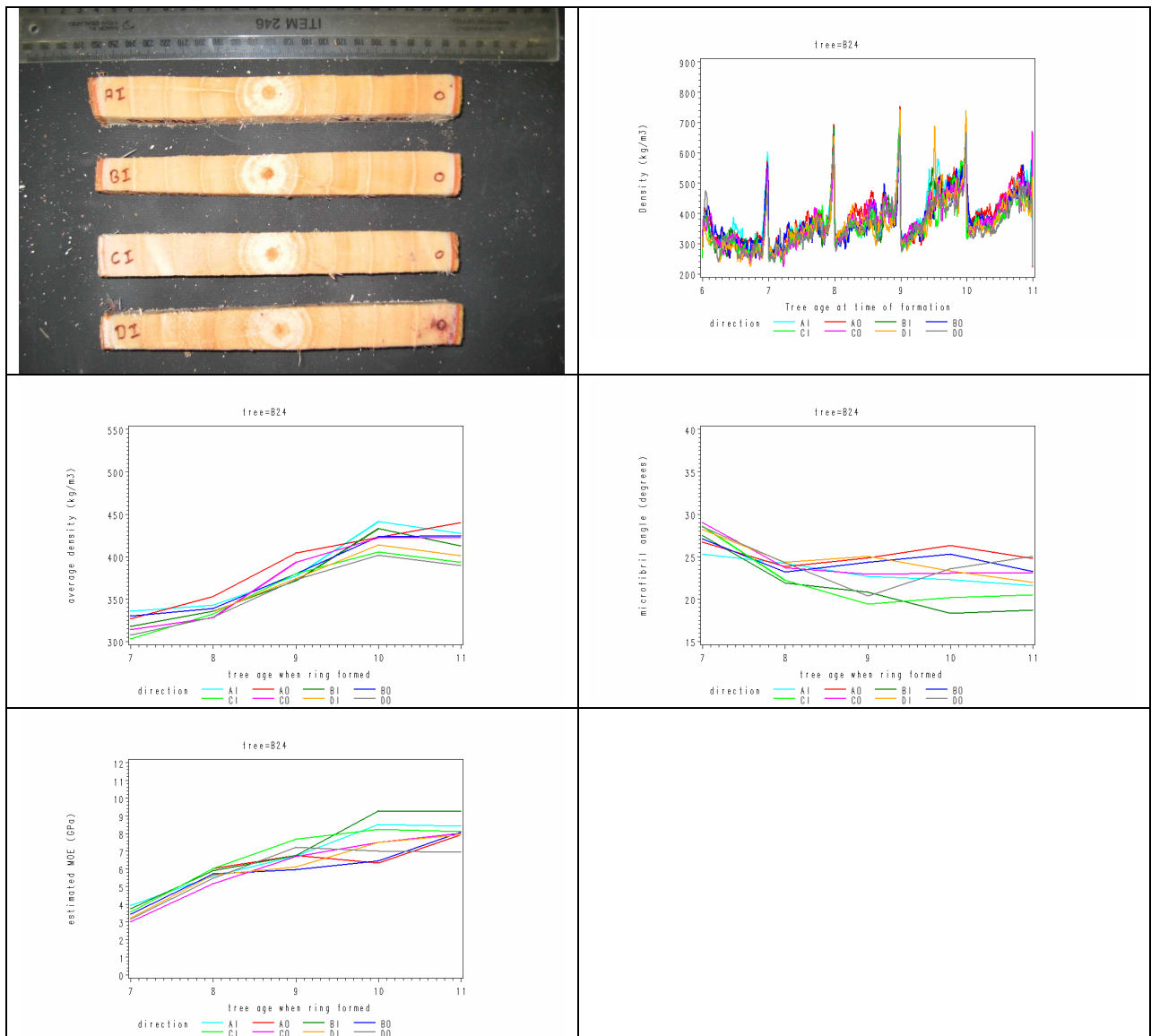
Appendix 4. Wood properties of samples saved from a long internode.

Wood samples were saved from two long swept internodes to observe how wood properties varied in the vicinity of a bend. The tables are laid out as follows:

Table 31. Layout of tables in Appendix 4.

Image of sample strips from internode.	SilviScan density profiles versus tree age at time of formation, i.e. all wood formed in one year is in the same horizontal position in the graph.
Ring average density (from SilviScan) versus tree age when the ring was formed.	Ring average microfibril angle (from SilviScan) versus tree age when the ring was formed.
Ring average longitudinal modulus of elasticity (from SilviScan) versus tree age when the ring was formed.	

Table 32. Tree B24: Samples from a long internode.

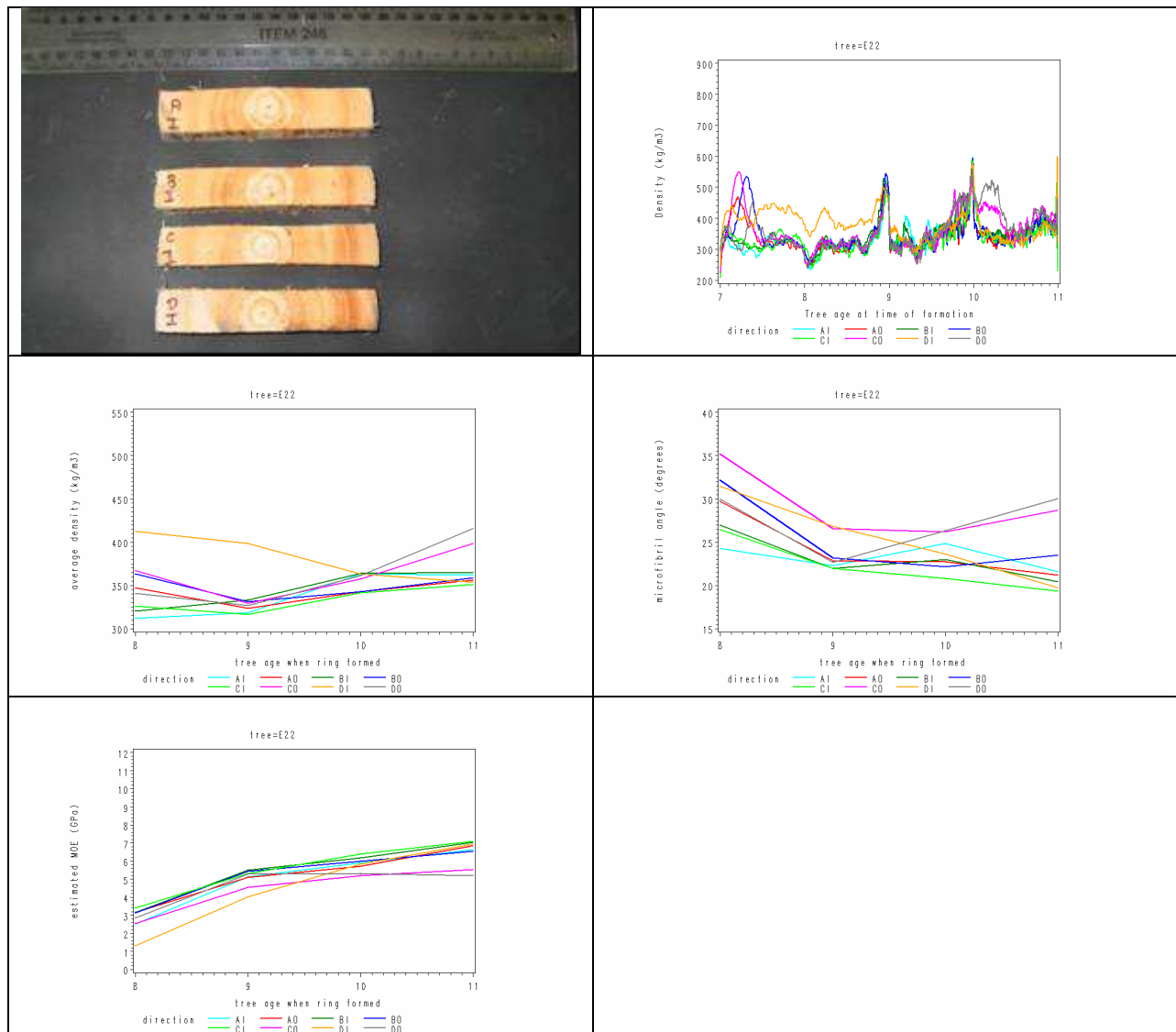


Comments

These 4 strips were approximately 20 cm apart. The maximum stem deviation across this stem section was approximately 2 cm.

At first glance, these samples show little variation in colour. Direction AO has slightly higher density and slightly higher MFA than the other samples. Directions BI and CI have lower MFA than the other directions.

Table 33. Tree E22: Samples from a long internode



Comments

These 4 strips were approximately 7 cm apart. The maximum stem deviation across this stem section was approximately 2 cm.

There are noticeable differences in colour (visible compression wood) between these different directions. Sample DI stands out as having very high density in the first two rings. The colour looks different from CI, but it is possible this is a lighting effect. Directions CO and DO have higher MFA in the last two rings. This corresponds with a darker colour.

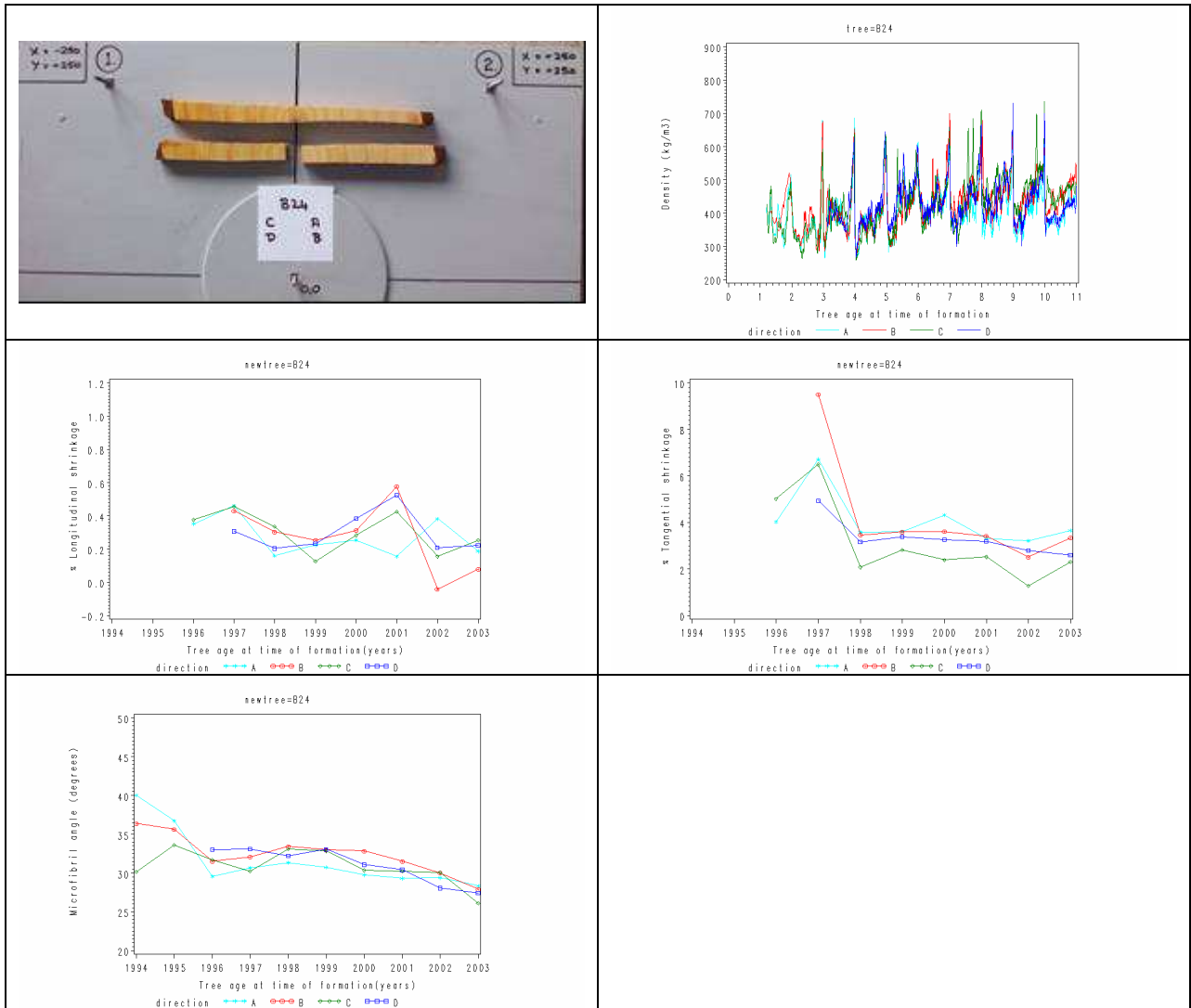
Appendix 5. Wood properties of ‘Shrinkage samples’.

These samples shown in Appendix 5 were taken from an internode near the base of a swept tree. The tables are laid out as follows:

Table 34. Layout of tables in Appendix 5.

Image of sample strips.	SilviScan density profiles versus tree age at time of formation, i.e. all wood formed in one year is in the same horizontal position in the graph.
Ring average density (from SilviScan) versus tree age when the ring was formed.	Ring average microfibril angle (from SilviScan) versus tree age when the ring was formed.
Ring average longitudinal modulus of elasticity (from SilviScan) versus tree age when the ring was formed.	

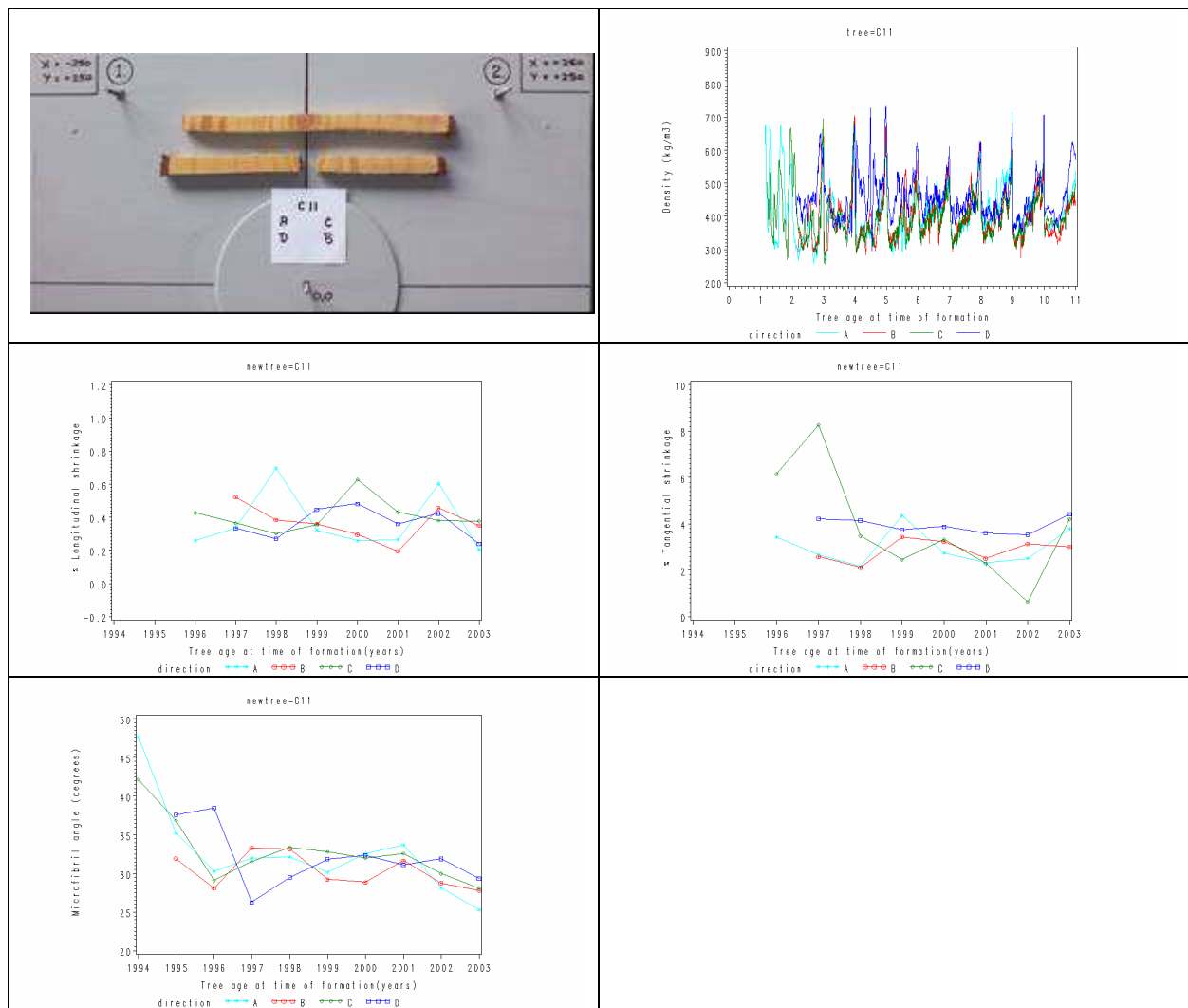
Table 35. Bent tree B24, selected disc 63-80 cm.



Note

The innermost ring on each sample may not be complete, and hence averages for that ring should be treated with caution.

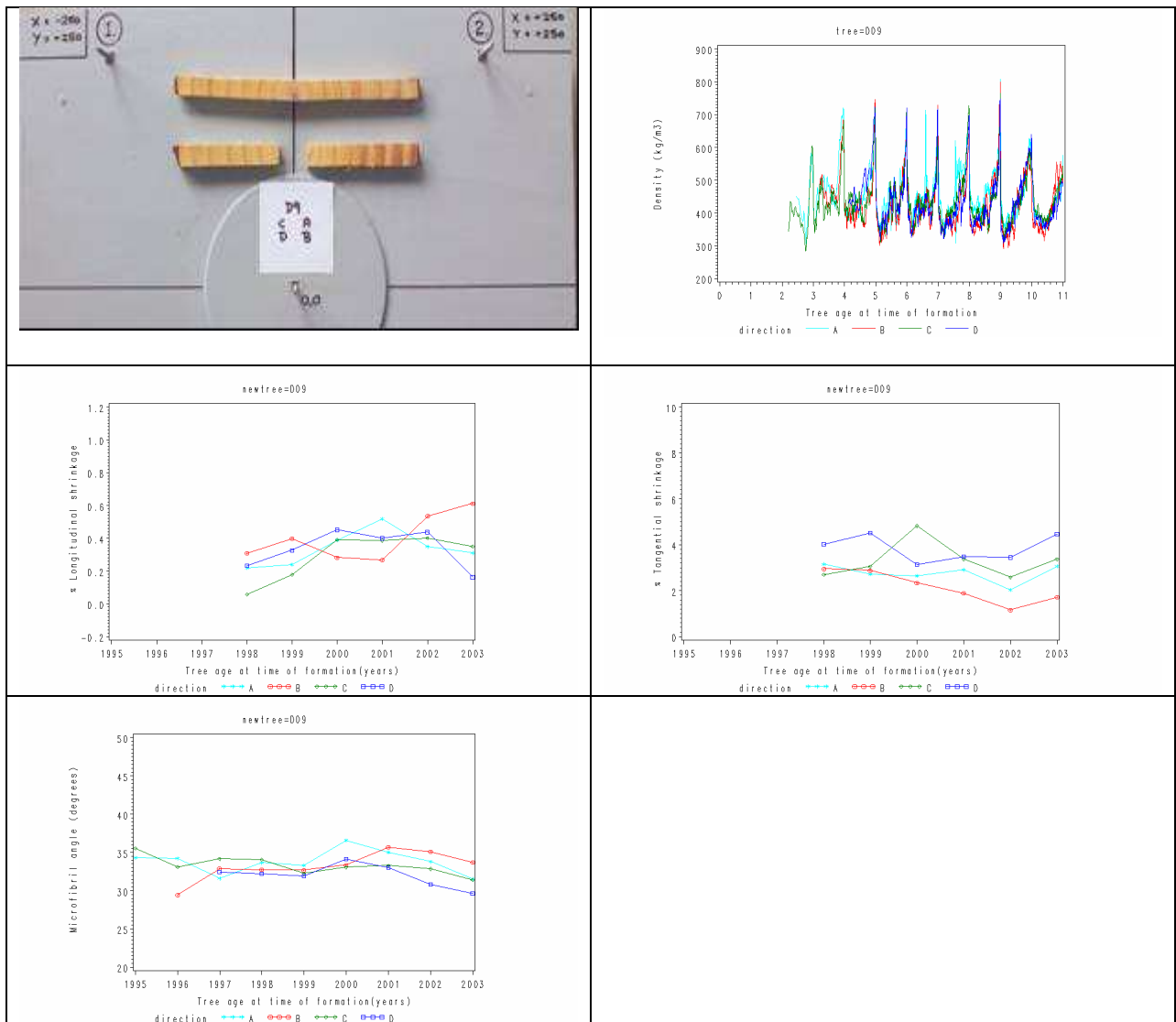
Table 36. Bent tree C11, selected disc 78-94 cm.



Note

The innermost ring on each sample may not be complete, and hence averages for that ring should be treated with caution.

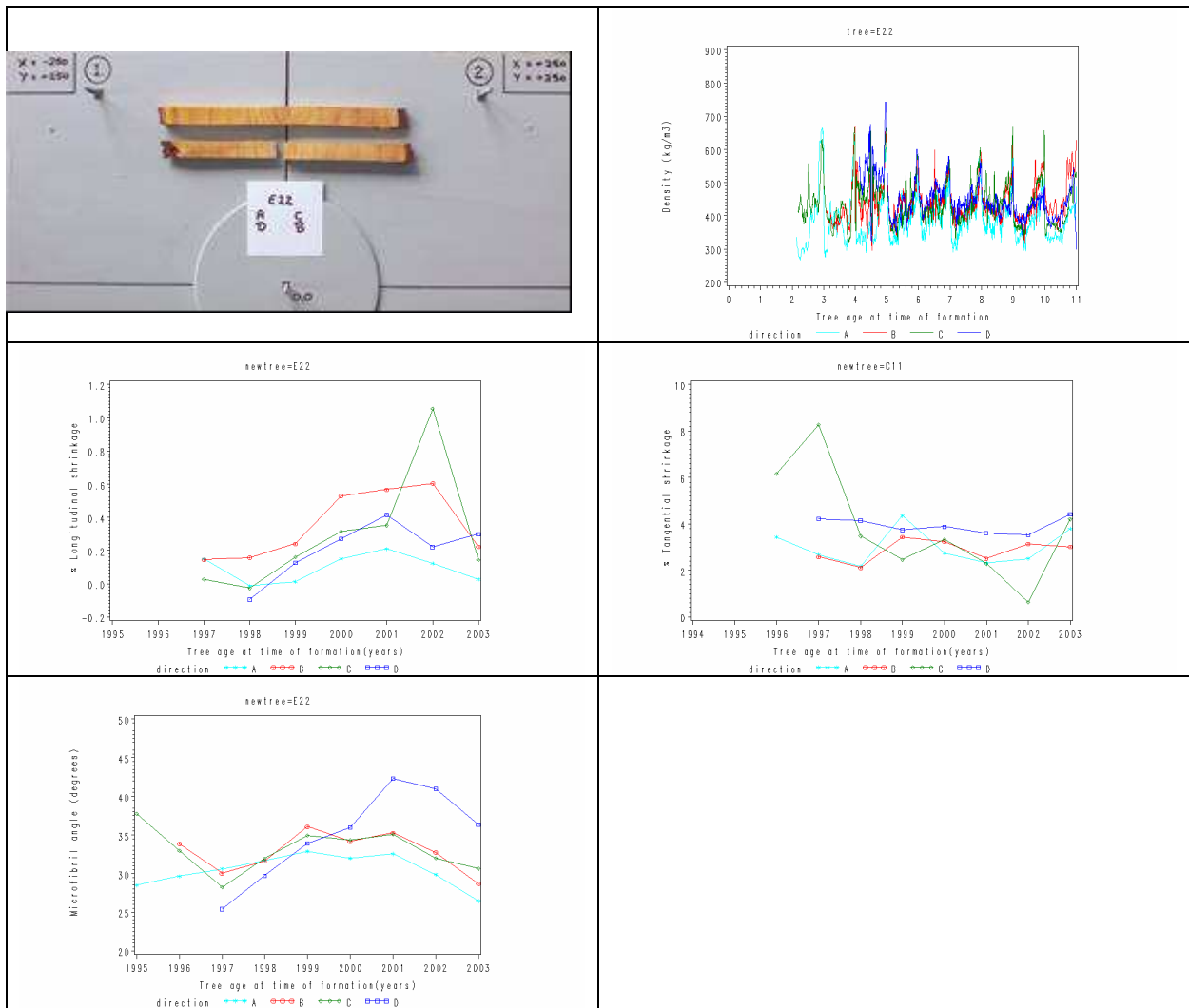
Table 37. Bent tree D09, selected disc 184-202 cm



Note

The innermost ring on each sample may not be complete, and hence averages for that ring should be treated with caution.

Table 38. Bent tree E22, selected disc 69-84 cm.

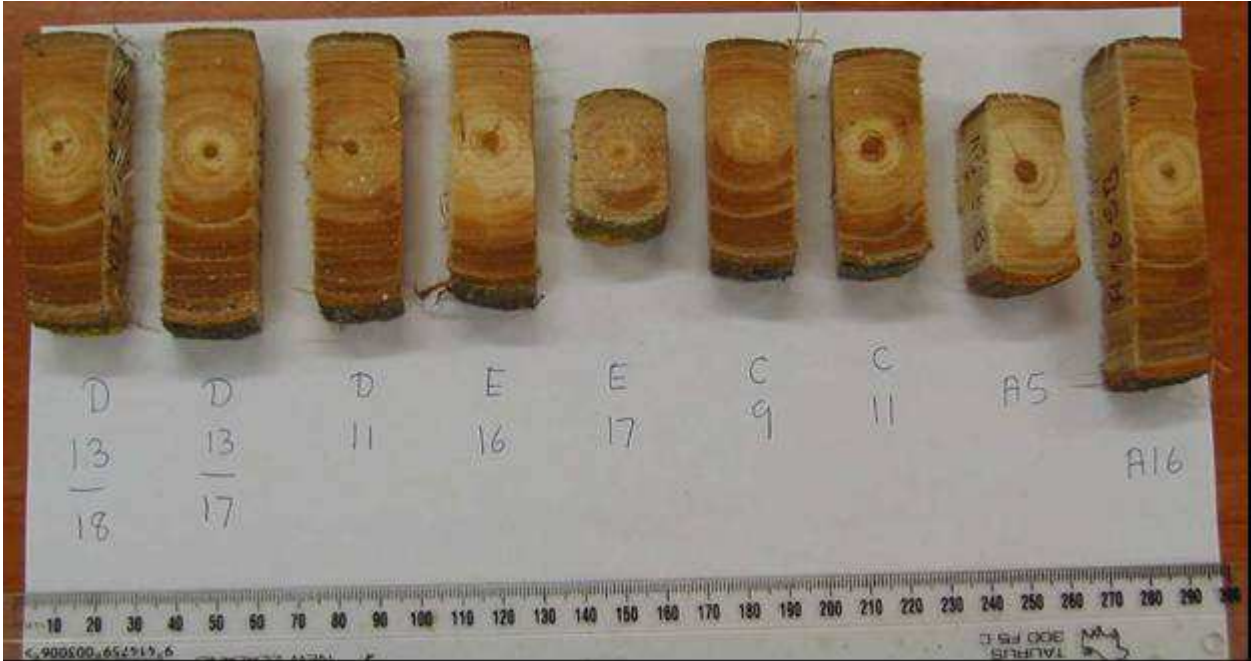


Note

The innermost ring on each sample may not be complete, and hence averages for that ring should be treated with caution.

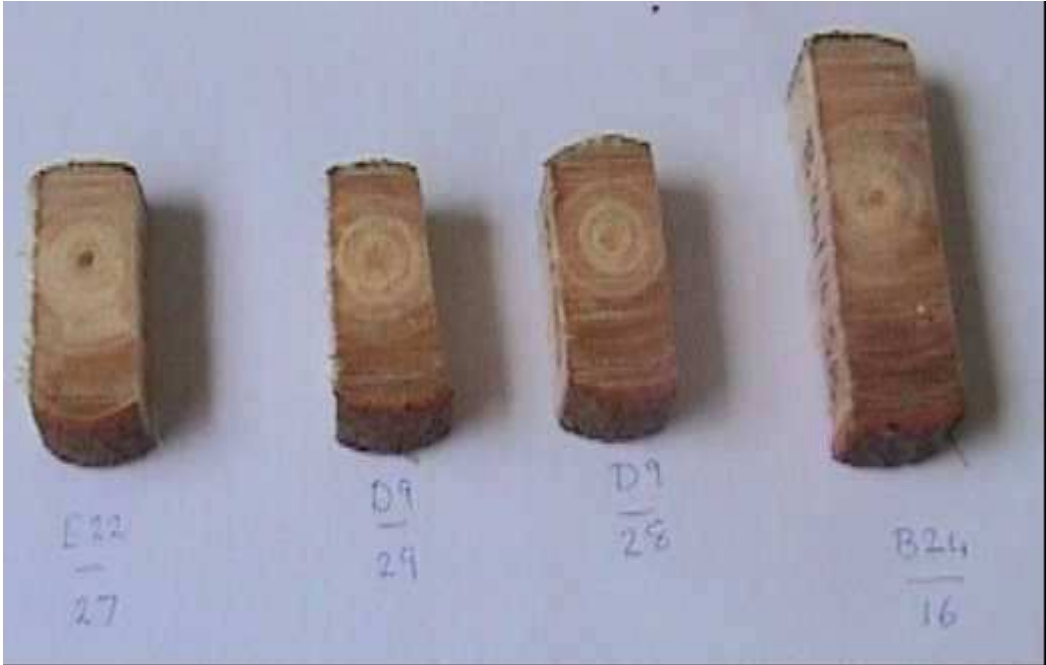
Appendix 6 Wood Properties – Branches

Figure 13. Branch samples sent for SilviScan analysis.



Note: labelling for each branch is “Plot label / Tree number / cluster number (if present)”.

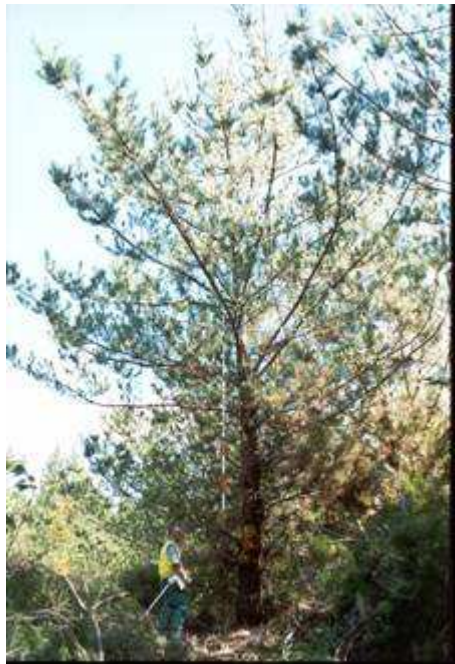
Figure 14. Branch samples sent for SilviScan analysis.



Note: Labelling for each branch is “Plot label+Treenummer/Cluster number”.

Appendix 7. PhotoMARVL images.

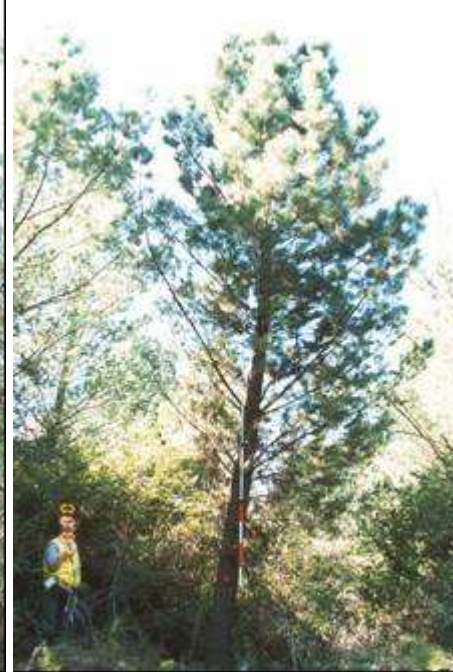
Table 39. PhotoMARVL Images for 4 of the bent trees.



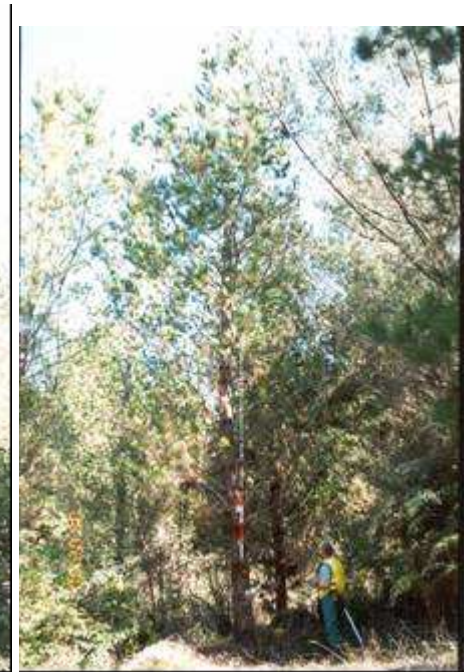
Tree B24



Tree C11



Tree D09



Tree E22